FRIEDRICH-ALEXANDER
UNIVERSITÄT
ERLANGEN-NÜRNBERG

TECHNISCHE FAKULTÄT

Department of Materials Science

Glass and Ceramics

ANNUAL REPORT 2015

Preface

In June 2015 we could welcome our new colleague Prof. Kyle G. Webber heading the functional ceramics department. Together with two research fellows from his DFG funded Emmy-Noether-Group he started his research activities in the field of ferroelectric ceramics. After transfer of unique experimental facilities from TU Darmstadt to FAU Erlangen his experimental equipment is ready for work.

In the glass department (Prof. Dominique de Ligny) research centers on a better understanding of light interaction with glass as well as response to external stress. Laser glass interaction is explored for new functionalization of glass by surface texturing. The disordered structure of glass imposes the development of specific instrumentation as vibrational spectroscopy. A new setup coupling Raman and Brillouin spectroscopy as well as a calorimeter allows new and unique prospective ways.

In the biomaterials department (Prof. Stephan E. Wolf), the DFG funded Emmy-Noether-Research Group on biomimetic materials started the research activities after completing the refurnishment of the laboratories. Work is focused on identifying the process-structure-property relationships in biominerals and subsequent in vitro mimesis by biomimetic crystallization at ambient conditions. Initial results were published in *Nature Communications* (see publications).

Work of the research group on cellular ceramics (Dr. Tobias Fey) is centered on microstructure characterisation applying X-ray microtomography and testing of the mechanical and thermal properties of cellular ceramics. Massive strain amplification lattice structures were investigated by experimental and theoretical approaches. In the generative ceramic processing group (Priv.-Doz. Dr. Nahum Travitzky) research activities envisage formation of multilayer refractory ceramics from preceramic paper. Electric sensor patterns were integrated by screen printing technologies.

Intensive cooperation with the Advanced Materials group at the Nagoya Institute of Technology, Japan, continued including several visits of Japanese colleagues to Erlangen and vice versa. Fortunately, we received the approval of a new DAAD funded exchange program on “Advanced Cellular Bioceramics” between FAU (WW 3) – Nagoya Institute of Technology, Japan and Sung Kjun Kwan University Suwon, Korea. With this program Master and PhD students as well as faculties coming to Erlangen as well as our fellows visiting the partners in Japan and Korea will be funded in 2016-2017.

The institute took part in the *2015 Lange Nacht der Wissenschaften* by presenting interesting results on the research in bioceramics, cellular and functional materials. We could celebrate the 40 years of continuous employment of Alfons Stielgeschmitt. Since October 2015 Prof. Greil serves as the dean of the faculty of engineering.

I want to express my sincere thanks to the members as well as to all friends of the institute of glass and ceramics.

Peter Greil

Outline

Team of the chair of glass and ceramics enjoying the annual excursion to Oberviechtach

1. INSTITUTE OF GLASS AND CERAMICS

a. Staff

Faculties

Prof. Dr. Peter Greil	Head of Institute
Prof. Dr. Dominique de Ligny	Glass
Prof. Dr. Kyle G. Webber	Functional Ceramics
Prof. Dr. Stephan E. Wolf	Biomimetic Materials
PD Dr. Nahum Travitzky	Ceramics Processing

Administration

Karin Bichler

Candice Iwai

Evelyne Penert-Müller

Senior Research Staff

Dr.-Ing. Ulrike Deisinger[1]	Ceramic Multilayer Processing
Dr.-Ing. Tobias Fey	Cellular Ceramics and Simulation

[1] *now in industry*

Research Staff

M. Sc. Azatuhi Ayrikyan

Dr. Guo Ping Bei[2]

M. Sc. Alexander Bonet

M. Sc. Corinna Böhm

Ph.D. Maria Rita Cicconi

Dr. Andrea Dakkouri-Baldauf

M. Sc. Benjamin Dermeik

M. Sc. Franziska Eichhorn

Ph.D. Xiaomeng Fan

M. Sc. Ina Filbert-Demut

M. Sc. Matthias Freihart

M. Sc. Zongwen Fu

Dipl.-Ing. Philipp Geiger

M. Eng. Michael Hambuch

M. Sc. Ruth Hammerbacher

Ph.D. Joseph Harris

Dipl.-Ing. Daniel Jakobsen

Dr. Barbara Kaeswurm

M. Sc. Hannes Lorenz

Dr. Kalina Malinova-Tonigold

Dr.-Ing. Joana Pedimonte

Dipl.-Ing. Lorenz Schlier[2]

Dipl.-Ing. (FH) Tobias Schlordt[2]

Dipl.-Ing. Alfons Stiegelschmitt

M. Sc. Martin Stumpf

Ph.D. Alexander Veber

M. Sc. Moritz Wegener

M. Sc. Bastian Weisenseel

Dipl.-Ing. Bodo Zierath

Technical Staff

Sabine Brungs

Timotheus Barreto-Nunes

Evelyn Gruber

Heiko Huber

Beate Müller

Heike Reinfelder

Peter Reinhardt

Eva Springer

Dipl.-Ing. Alfons Stiegelschmitt

Hana Strelec

Andreas Thomsen

[2] *now in industry*

Excursion to the lead crystal glass production lines of Nachtmann GmbH (Weiden) followed by a guided hike through old gold mining areas with gold panning in a creek (Oberviechtach)

Welcome to Professor Dr. Kyle G. Webber

Kyle G. Webber, born in 1980, graduated in Marine Systems Engineering from Maine Maritime Academy in 2003, where he also received his United States Coast Guard License for a 3rd Assistant Engineer for steam, diesel, or gas turbine vessels of unlimited horsepower. In 2005 and 2008, respectively, he received a M.Sc. and Ph.D. in Mechanical Engineering from the Georgia Institute of Technology for his work on the nonlinear electromechanical constitutive behavior of single crystal and polycrystalline ferroelectric materials. In 2008, he joined the Department of Material- and Geosciences at the Technische Universität Darmstadt as a postdoctoral researcher investigating the mechanical properties of ferroelectrics, such as high temperature ferroelasticity, stress-induced phase transformations, and fracture. In 2014, he was appointed as a Junior-Professor at the Technische Universität Darmstadt, heading the *Electromechanics of Oxides* research group.

In 2013 he was awarded a Emmy Noether Research Grant by the Deutsche Forschungsgemeinschaft on "*The Influence of Mechanical Loads on the Functional Properties of Perovskite Oxides*". Perovskite-structured ceramics are commercially important oxide ceramics that are used in numerous actuation, sensing, and energy applications due to their wide-ranging functional material properties, such as ferroelectricity, ferromagnetism, superconductivity, colossal magnetoresistance, and ionic conductivity. The aim of this project is to investigate the influence of mechanical loads on two advanced applications: large displacement actuators and cathode materials for solid oxide fuel cells, which involves stress-modulated structural phase transformations and ionic conductivity.

b. Equipment

Technical hall (600 m²): equipped with facilities for advanced processing, shaping, melting, and sintering as well as molding of glass, ceramics and composites

Main Equipment

Laboratories

- Biomaterials laboratory
- Ceramography workshop
- Functional ceramics laboratory
- Glass laboratory
- Mechanical testing laboratory
- Multilayer processing laboratory
- Polymer processing laboratory
- Powder characterization laboratory
- Processing workshop
- Rapid Prototyping laboratory
- SEM/AFM laboratory
- Simulation laboratory
- X-ray characterization laboratory

Equipment

Thermal analysis

- 3-dimensional optical dilatometer
- Push rod dilatometers (up to 1800 °C)
- Thermal analysis (DTA/TGA/DSC/TMA)
- Thermal conductivity devices
- Viscometry (beam bending)

Powder characterization

- ESA acoustophoretic analyser (Zeta-meter)
- Dynamic light scattering particle size analyser
- Gas absorption analyser (BET)
- Laser scattering particle size analyser
- X-ray diffractometers (high-temperature)

Optical analysis

- FT-IR spectrometer
- High-resolution fluorescence spectrometer
- Light Microscopes (digital, polarization, in-situ hot stage)
- Scanning electron microscope (variable pressure, ESEM and high temperature with EDX)
- UV-VIS-NIR spectrometers

Drying stress measurements

- High precision mechanical testing with optical tracking system (EXAKT)
- Impulse Excitation Measurement (buzz-o-sonic)
- Micro hardness tester
- Servo hydraulic mechanical testing systems (also high temperature)
- Single fibre tensile testing machine
- Viscosimeter and elevated-temperature viscosimeter

Chemical analysis

- ICP-OES (Spectro Analytical Instruments)

Structural analysis

- 2D laser scanning microscope (UBM)
- 3D Laser scanner
- Atomic force microscope (AFM)
- Electron paramagnetic resonance spectroscopy
- He-pycnometer
- High accuracy weighing scales
- Laser-Flash LFA 457
- Mercury porosimeter
- Micro-CT Sky scan 1172
- Microwave and ultrasonic devices for non-destructive testing
- Raman-microscope with two excitation lasers

Powder and slurry processing

- Attrition mills
- Agitator bead mill
- Disc mill
- Intensive mixers (Eirich, powder and inert gas/slurry)
- Jaw crusher
- Overhead mixers
- Pick and Placer
- Planetary ball mills
- Planetary centrifugal mixer (Thinky)
- Rotary evaporators
- Sieve shakers
- Single ball mill
- Thermo kneader
- Three-roll mill
- Tumbling mixers
- Ultrasonic homogenizer

- 3D printers
- Advanced screen printing device
- Calender
- CNC High speed milling machine
- Cold isostatic press
- Electrospinning machine
- Flaring cup wheel grinding machine
- Fused deposition modelling device (FDM)
- High precision cutting device
- Hot cutting device
- Laminated object manufacturing devices (LOM)
- Lamination presses
- Langmuir–Blodgett trough
- Lapping and polishing machines
- Low-pressure injection moulding machine
- Plate shear for cutting thick green sheets
- Positioning unit with a resolution of +/- 35 microns
- Precision diamond saws
- PVD coaters
- Robot-controlled device
- Roller coater
- Screen printer
- Sheet former
- Spin coater
- Tape caster
- Textile weaving machine
- Twin screw extruder
- Ultrasonic drill
- Vacuum infiltration device

Heat treatment

- Autoclave
- Dryers
- Furnaces (air, N_2, Ar, Vac, High-Vac, forming gas) up to 2500°C for sintering, glass melting, infiltration, debindering, pyrolysis
- Gradient furnace
- High-temperature spray furnace

Prof. Dr. Peter Greil congratulates Dipl.-Ing. Alfons Stiegelschmitt for 40 years of service

c. International

Visiting Students and Scientists

Prof. Dr. Shangwu Fan (February 2014 – February 2015)
Northwestern Polytechnical University, Xi'an, P.R. China

Hyuen Woo Yang (January 2015 – February 2015)
Sungkyunkwan University (SKKU), South Korea

Jina Yang (January 2015 – February 2015)
Sungkyunkwan University (SKKU), South Korea

Jimei Xue (March 2015 – August 2015)
Northwestern Polytechnical University, Xi'an, P.R. China

Hatim Laadoua (April 2015 – July 2015)
Ecole Nationale Supérieure d'Ingénieurs de Limoges (ENSIL), Limoges, France

Sana Rachidi (May 2015 – August 2015)
Ecole Nationale Supérieure d'Ingénieurs de Limoges (ENSIL), Limoges, France

Julie Pradas (June 2015 – September 2015)
Ecole Nationale Supérieure d'Ingénieurs de Limoges (ENSIL), Limoges, France

Prof. Dr. Jean Rocherullé (July 2015)
Université Rennes 1, France

Prof. Dr. Ronan Lebullenger (July 2015)
Université Rennes 1, France

Dr. Franck Tessier (July 2015)
Université Rennes 1, France

Prof. Dr. Dorrit Jacob (August 2015)
ARC Centre of Excellence for Core to Crust Fluid Systems and GEMOC ARC National Key Centre, Department of Earth and Planetary Sciences, Macquarie University, Sydney, Australia

Takahiro Fujiwara (November 2015)
Nagoya Institute of Technology, Ceramic Research, Nagoya, Japan

 0

Takahiro Fujiwara during his visit to our institute in November 2015

2. RESEARCH

a. Project List

Research centres on basic aspects of ceramics, glasses and composites. Materials for applications in microelectronics, optics, energy, automotive, environmental, chemical technologies and medicine were investigated. Research was carried out in close cooperation with partners from national and international universities and industries.

Research Projects (in alphabetical order)	**Funding**	**Principal Investigator**
BayFOR Australia „Variable Crystallinity in Natural and Synthetic Nanocomposite Materials“	BayFOR	S.E. Wolf
Bioactive ceramic cages	IN	P. Greil / T. Fey
Cellular ceramics for heat absorbers	EnCN	P. Greil
Deformation and sintering behaviour of preceramic papers	DFG	N. Travitzky
Development of layered structures and 3D generative processing methods for innovative combustion chamber lining concepts	BMWi + IN	A. Roosen / N. Travitzky
Dispers systems for electronic devices	DFG	A. Roosen
Emmy Noether Programme “The Influence of Mechanical Loads on the Functional Properties of Perovskite Oxides”	DFG	K.G. Webber
Environmentally friendly development of white phosphorus on the basis of oxynitride phosphate glasses.	BFHZ	D. de Ligny

Evaluation of the densification mechanism during realisation of dense ceramic layers at room temperature via the Aerosol Deposition Method	DFG	K.G. Webber
Experimental study and simulation of anisotropic effects in cast green tapes	DFG	A. Roosen
Flexible manufacturing of preceramic paper based refractory components	DFG	P. Greil
Formation of Liquid-condensed mineral phases and the mechanisms of the PILP process (Emmy Noether Group)	DFG	S.E. Wolf
Hierarchical cellular ceramics and composites	DFG	P. Greil
High coordination numbers: topo-structural implication on glass strength	DFG	D. de Ligny
High temperature stable ignition components based on defined 2D and 3D SiSiC structures	AiF	N. Travitzky
Integrated Calorimetry and Vibrational Spectroscopies	DFG	D. de Ligny
Lightweight cellular ceramics	EC	P. Greil
Manufacture of scaffolds for tissue engineering applications in rapid prototyping techniques	BMBF	P. Greil
Manufacturing of multilayer refractories by tape casting	DFG	A. Roosen
Robocasting of macrocellular ceramic 3D-lattice structures with hollow filaments	DFG	N. Travitzky

Self healing MAX phase ceramics	DFG	P. Greil
Stable and metastable multiphase systems for high application temperatures	DFG	P. Greil
Structured carbon based catalyst support structures for CO hydration	DFG	T. Fey
Tape-on-Ceramic Technology	BMBF	A. Roosen
Towards smart solar cell glasses: Glass texturing under laser irradiation	EnCN	D. de Ligny

Funding organizations:

AiF:	Industrial research Cooperation
BayFOR:	Bavarian Research Alliance
BFHZ:	Bavarian-French Academic Centre
BMBF:	Federal Ministry of Education and Research
BMWi:	Federal Ministry of Economics and Technology
DFG:	German Research Foundation
EC:	Cluster of Excellence (“Engineering of Advanced Materials”)
EnCN:	Energy Campus Nuremberg
IN:	Industry

b. Selected Research Highlights

Mechanical and Electrical Strain Response of a Piezoelectric Auxetic PZT Lattice Structure

Tobias Fey, Franziska Eichhorn, Guifang Han, Kathrin Ebert, Moritz Wegener, Andreas Roosen, Ken-ichi Kakimoto, Peter Greil

A two-dimensional auxetic lattice structure was fabricated from a PZT piezoceramic. Tape casted and sintered sheets with a thickness of 530 µm were laser cut into inverted honeycomb lattice structure with re-entrant cell geometry (θ = - 25°) and poling direction oriented perpendicular to the lattice plane. The in-plane strain response upon applying an uniaxial compression load as well as an electric field perpendicular to the lattice plane were analyzed by a 2D image data detection analysis. The auxetic lattice structure exhibits orthotropic deformation behavior with a negative *in-plane* Poisson´s ratio of -2.05. Compared to PZT bulk material the piezoelectric auxetic lattice revealed a strain amplification by a factor of 30 – 70. Effective transversal coupling coefficients d^{al}_{31} of the PZT lattice exceeding $4 \cdot 10^3$ pm/V were determined which result in an effective hydrostatic coefficient d^{al}_{h} 66 times larger than that of bulk PZT.

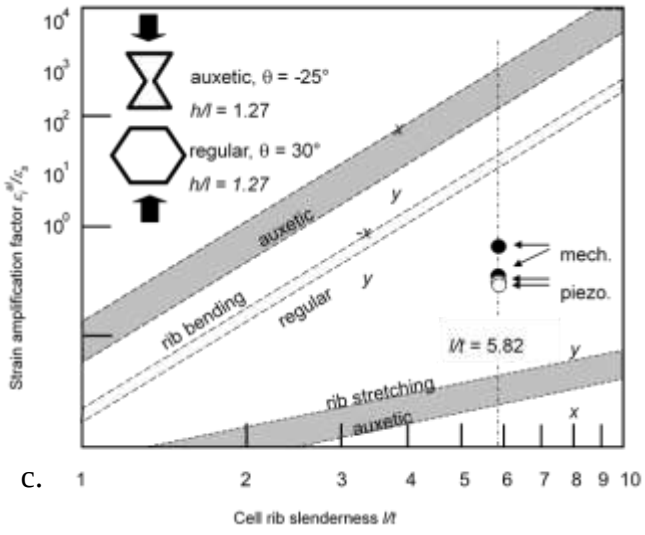

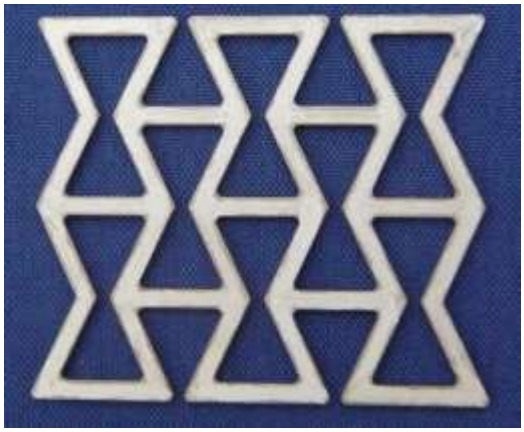

Microstructural, mechanical and thermal characterization of alumina gel-cast foams manufactured with the use of agarose as gelling agent

Tobias Fey, Bodo Zierath, Peter Greil, Marek Potoczek

Alumina gel-cast foams manufactured by using agarose as gelling agent were examined in terms of microstructural, mechanical and thermal properties. The microstructural SEM measurements of alumina foams were compared with X-ray micro tomography investigations also on the pore network. Young's Modulus of alumina foams was determined of impulse excitation and ultrasonic sound velocity measurements. These two independent techniques showed similar results. Gibson and Ashby's s model of completely open-cell and closed-cell foams was compared with experimental data derived from compression tests. The thermal conductivity measurements using Laser-Flash Analysis were correlated with the pore network in the alumina foam structure.

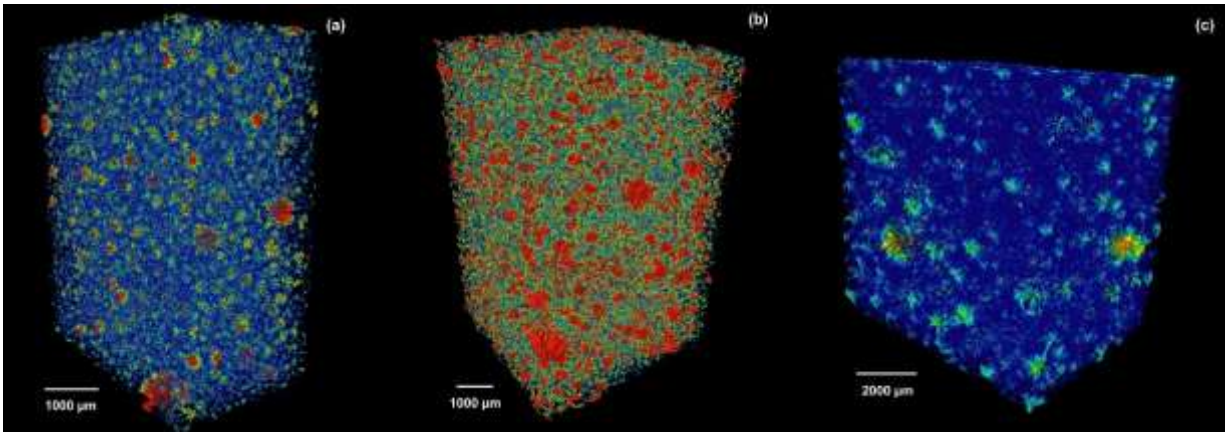

3D-visualisation of pore network at a) 60% , b) 77% and c) 89% porosity

Chemical tunability of europium emission in phosphate glasses

Maria Rita Cicconi, Alexander Veber, Dominique de Ligny

The development of new generation of low-energy lighting is closely related to the properties of the phosphors used. They must fulfill several criteria: color, emission efficiency and ease of production. In the case of white LED (WLED) it is mainly done using the Ce^{3+} as a dopant in the YAG associated with GaN-type blue LED. Most of the time in this case the phosphor is obtained at high temperatures under reducing conditions, around 1400 ° C, by reaction in the solid state. The powders obtained have a low crystallinity and do not allow the production of large size transparent parts. Moreover, after use the recycling of rare earth is very difficult. Its environmental footprint presents two bad points: a high production energy cost and an almost non reuse after lifetime. Even if the emission spectrum of such a YAG:Ce WLED is nearly continuous, an overrepresentation from the blue LED emission makes the light slightly cold. We developed a white emission phosphor based on an oxynitride phosphate glass. In this case, rare earth Eu which was used in its reduced form Eu^{2+} has a continuous emission spectrum limited to the visible (Fig 1.). An advantage of phosphate glasses is their very low synthesis temperatures, just few hundred degrees Celsius thus limiting the production energy costs. Moreover, a nitrification step allows us to improve both the durability properties of the glass and to further reduce the usual Eu^{3+} to its desired reduced Eu^{2+} form ensuring then a white emission spectrum (Fig 2.).

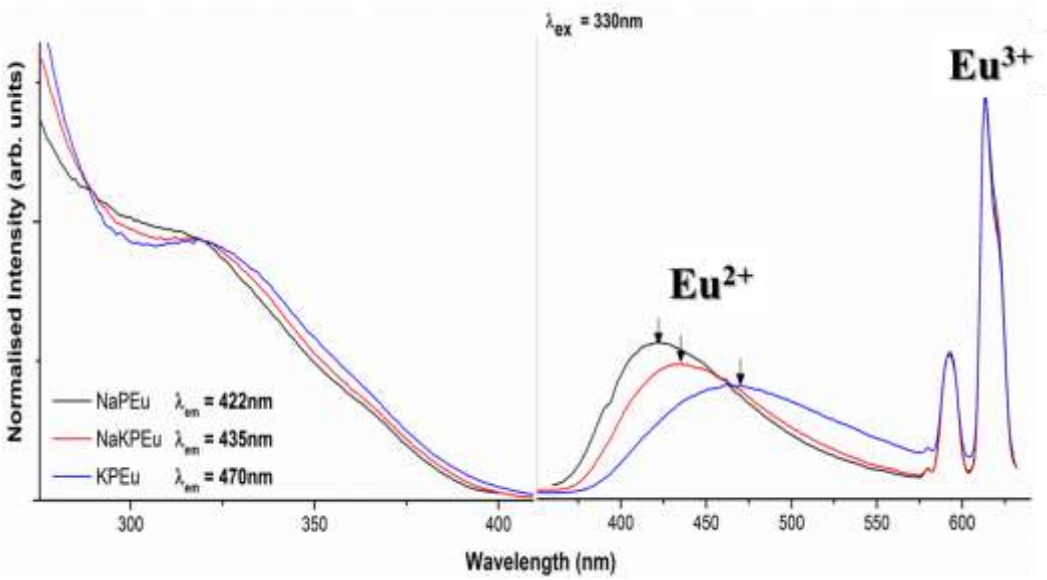

Fig. 1: Excitation and Photoluminescence spectra for Eu-doped phosphate glasses. Both Eu^{2+} emission and excitation bands shift toward red by substituting K for Na

As to further improve the glass formation ability and test chemical tunability glasses with Na, mixed Na-K and K were prepared. The photoluminescence studies clearly show that Eu^{2+} emission band shifts toward red by substituting the alkali cation, in the order Na<NaK<K, whereas the luminescence data here obtained suggest the presence of Eu^{3+} in just one site distribution. The large shift toward higher wavelengths, observed for samples synthetized in air, indicates that the network modifier ions strongly affect the nature of the Eu^{2+}-O bond, and so able a good tunability (Fig. 1).

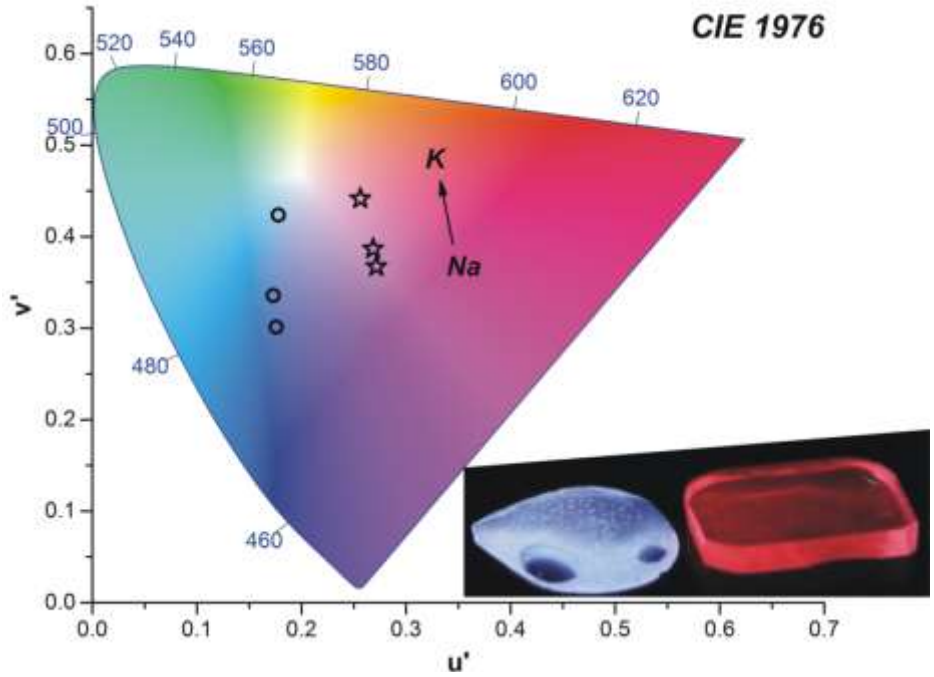

Fig. 2: CIE 1976 chromaticity diagram for the alkali-bearing phosphate glasses synthetized in air (stars) and under NH_3-flux (circles). The emission can be systematically tuned by changing the chemistry. In the inset the different luminescence for the NaKPEu glass synthesized in air (red) and under NH_3-flux (blue)

The first results of this study are very promising as well on the emission properties that the production energy saving obtained. In addition the glass technology, chosen here, can be considered for molding transparent parts in large volume, currently inaccessible by ceramic processes. As in nature apatite crystallization at the end of the LED life cycle will help the Eu recovering.

This study is realized in collaboration with Jean Rocherullé, Ronan Lebullenger and Franck Tessier of Rennes University, France and received the support of the Bayerisch-Französisches Hochschulzentrum (BFHZ).

Integrated Calorimetry and Vibrational Spectroscopies

Alexander Veber, Maria Rita Cicconi, Dominique de Ligny

The new equipment developed this year with vibrational spectrometer from 0,01 to 4000 cm^{-1} allows a fully multiscale approach of materials. In such experiment the calorimeter gives the energetic response of matter and the vibrational spectrometers observe its elastic and structural evolution. From 0,01 to 10 cm^{-1} the Brillouin inelastic scattering is sensitive to long range order properties like volume and elastic moduli. From 5 to 200 cm^{-1} the Raman Terahertz inelastic scattering is related to intermolecular bonds and from 200 to 4000 cm^{-1} to internal molecular vibrations (Fig 1).

Fig.1: Brillouin and Raman spectra of silica glass. Two pairs of peaks in Brillouin spectrum correspond to longitudinal and transverse acoustic waves in the glass. Raman spectra above 200 cm^{-1} originates from structural units of the glass network and below to vibration within the mid-range order

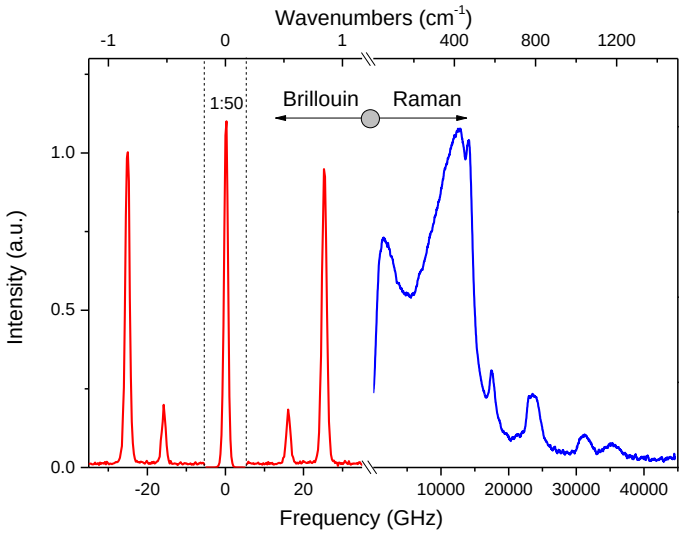

Doing these observations simultaneously in situ is useful to study any transition that implies several order parameters or exhibit relaxation phenomena. For example, they will help to understand phenomena as different as order–disorder phase transition, glass transition or crystallization. Its use is not restricted to glass and prospective projects are expected in the field of ceramic, mineralogy, polymers as well as more fundamental study for example of emulsions.

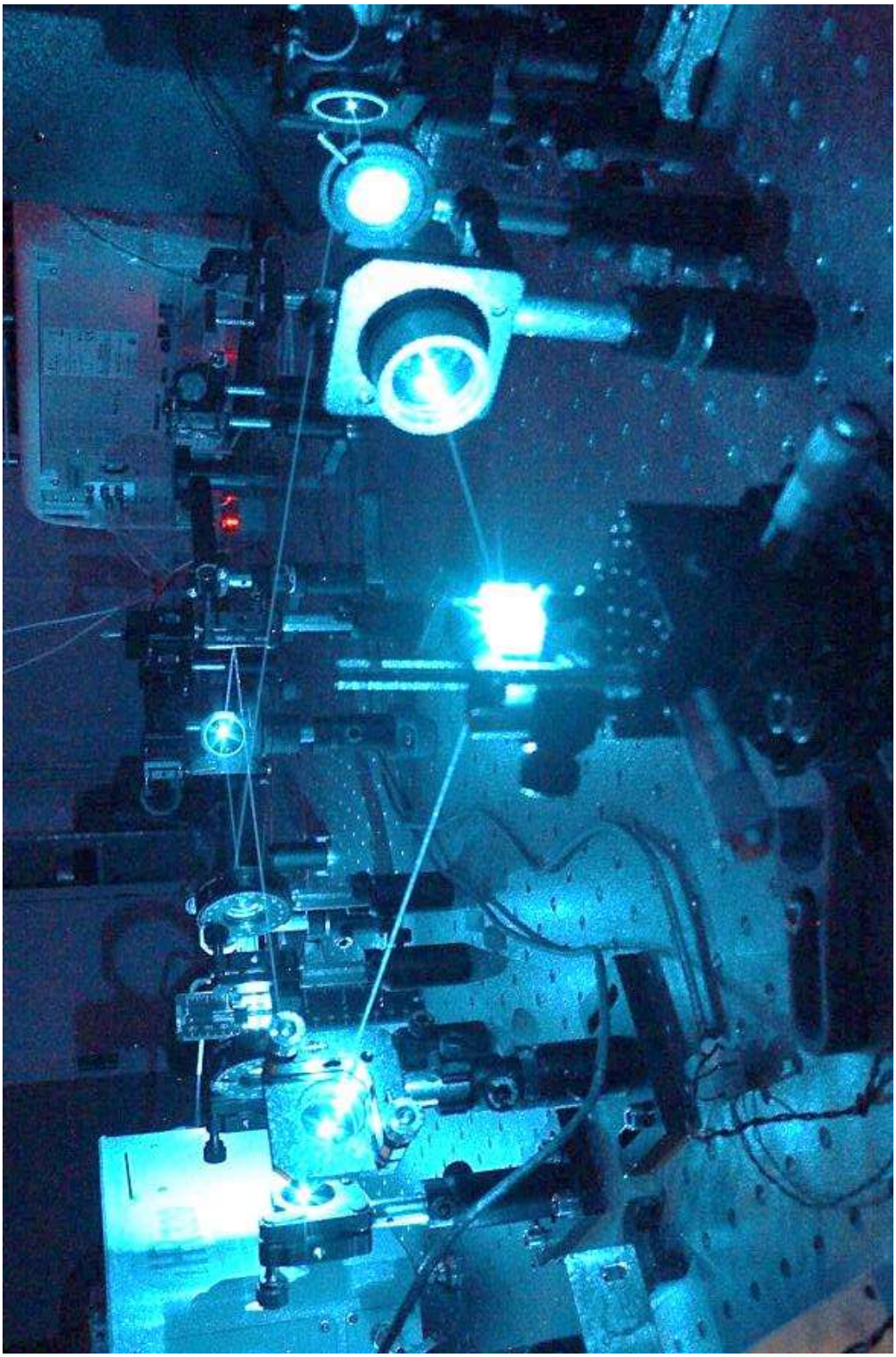

Integrated Calorimetry and Vibrational Spectroscopies setup using a 488 nm solid laser. The laser path between each equipment can be modulated in function of the needs.

Such tool unthinkable in the past is now possible due to new technologic improvements especially: the new 3D Bragg gratings, that allow easier recording of Raman spectra in the 5 to 200 cm^{-1} region, high sensitivity cameras with a better quantum efficiency allowing quick data recording in the same time scale that the calorimetric measurements, narrow intense solid lasers at low wavelength 488 nm to avoid black body emission but with enough power.

This setup was designed around the path of the laser as shown in Fig. 2. By adjusting all the equipment on an optical table, a robust and versatile design was obtained. The path of light can be modified easily to get the better performances.

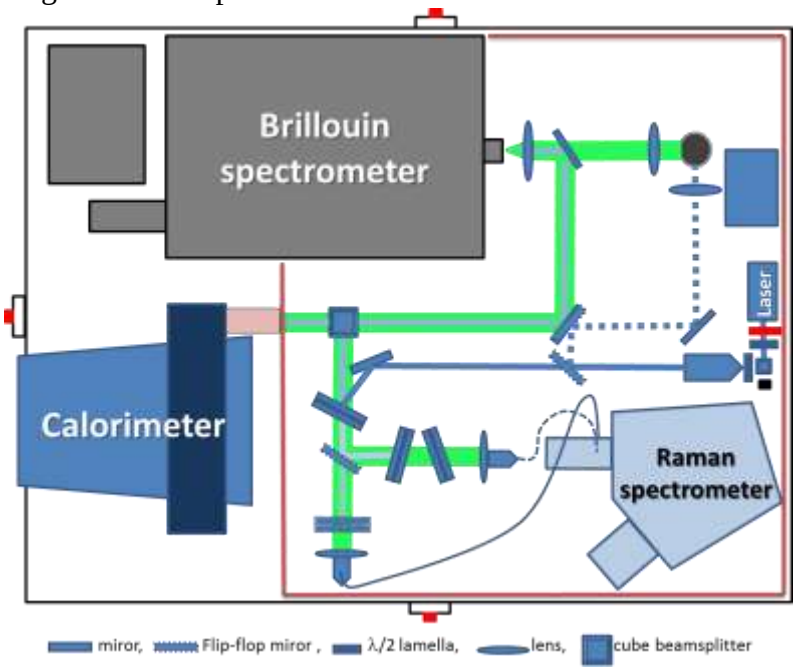

Fig 2: Path of the laser in blue and the backscattered signal in green. Macroscopic samples can be studies under different geometry by following the dash blue line and setting the sample at the grey circle

The sample can be observed as well macroscopically that in a microscope environment.

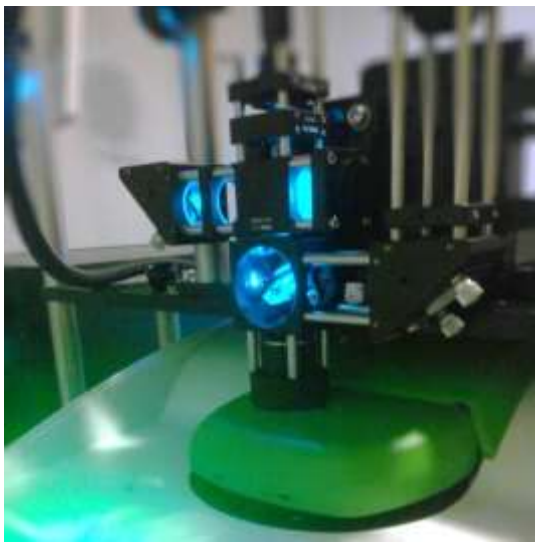

The microscope built around the DSC allows seeing the sample and the position of the laser on it at any time so quick adjustment can be realized. The spatial resolution can be low as a pair of microns using the x50 objective. The environment around the sample can be changed in the calorimeter between -70°C and 650°C with diverse atmosphere from inert to oxidizing.

Mechanical stability of polar defects in ferroelectric perovskites

Kyle G. Webber

One of the central advantages of the simple ABO_3 structure is the ability to significantly alter the functional properties with relatively small amounts of aliovalent and isovalent substitutions. Often, in the case of ferroelectric materials, aliovalent transition metals or rare-earth ions are selected that occupy either an A- or B-site, resulting in the formation or elimination of oxygen vacancies for charge compensation. Acceptor-doping with lower valence ions leads to the formation of oxygen vacancies ($V_O^{\cdot\cdot}$), which has been shown to electrically "harden" the ferroelectric and result in aging. These effects correspond closely to the development of an apparent internal bias electric field that depends on the concentration content as well as the thermoelectrical history of the sample. It is generally agreed that the observed enhancement in electromechanical properties and decreased electric poling fields in donor-doped ferroelectrics is correlated with the decreased oxygen vacancy content, the formation of A-site vacancies, and changes in B-site valance. This facilitates increased domain wall motion and, therefore, increased extrinsic contributions to the electromechanical properties.

Understanding the role of mechanical fields on acceptor-doped ferroelectrics is important, as many applications apply mechanical loads during operation. Therefore, the primary aim of this work is to investigate role of stress on donor- and acceptor-doped $Pb(Zr,Ti)O_3$ through the characterization of the stress- and temperature-dependent direct piezoelectric response. The samples used in this study are commercially available *soft* and *hard* PZT, which are both near the morphotropic phase boundary on the tetragonal side and have the following compositions: $Pb_{0.99}[Zr_{0.45}Ti_{0.47}(Ni_{0.33}Sb_{0.67})_{0.08}]_{1.00}O_3$ and $Pb_{1.00}[Zr_{0.47}Ti_{0.48}(Mn_{0.33}Sb_{0.32}Nb_{0.33})_{0.05}]_{1.00}O_3$, respectively. Mn^{2+} acts as an acceptor-dopant on the B-site, whereas Nb^{5+} is a donor dopant.

Measurement of the temperature- and stress-dependent longitudinal direct piezoelectric coefficient d_{33} was performed on a screw-driven load frame fitted with a heating chamber and custom-built equipment capable of applying small mechanical impulses at various frequencies. The load frame applied the global bias uniaxial compressive stress, while an integrated piezoelectric stack actuator, positioned in series with the sample and controlled by a LabVIEW program, partially unloaded the sample with a sinusoidal mechanical signal.

During testing a load amplitude of ±0.5 MPa was used. The small signal direct piezoelectric coefficient was calculated from the measured amplitudes of stress and polarization in a frequency range between 50 mHz and 240 Hz with an accuracy of better than ±0.2 pC/N.

The direct piezoelectric coefficient of the soft and hard compositions was determined during uniaxial compressive loading and unloading in the frequency range between 50 mHz - 240 Hz and is shown in Fig. 1. The arrows indicate the direction from lower frequencies to higher frequencies. The soft material displays a significantly larger $d_{33}d_{33}$ value, 550 to 600 pC/N, depending on frequency, in the poled state without applied stress. In contrast, the hard PZT composition has a d_{33} of 250 to 280 pC/N over the same frequency range. The lower piezoelectric response of hard PZT is due to the decrease in domain wall mobility and a subsequent decrease in the intrinsic contribution. With an increasing compressive stress, the piezoelectric response of the soft PZT is found to monotonically decrease above approximately -25 MPa, which is related to the first deviation from the linear elastic behavior (Fig. 1a). This point is where ferroelastic domain reorientation begins and is defined as the onset stress (σ_0). As the external compressive stress reorients domains parallel to polarization direction, the average piezoelectric response of the polycrystal decreases. This effect continues until saturation, where no additional domains are available to be switched. In comparison, the hard PZT displays an initial increase in d_{33} until -75 MPa, followed by a decrease and subsequent saturation. The initial increase is proposed to be due to the presence of an internal bias field created during the electrical poling process. As the applied bias stress increases, the electrostatic and mechanical forces work antagonistically and result in an increase in the piezoelectric response through enhanced domain wall motion. Further increases in the mechanical load see a shifting of this balance and a mechanical clamping of domains.

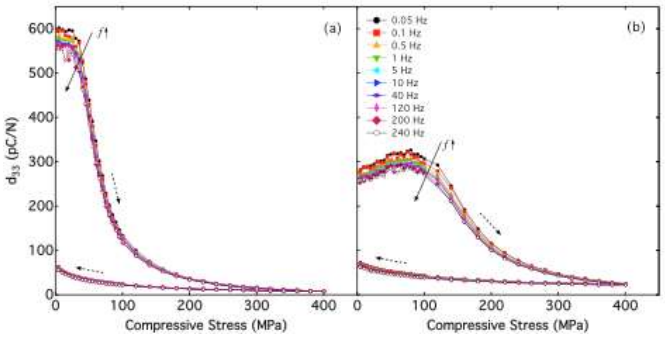

Fig. 1: Frequency-dependent piezoelectric coefficient with compressive bias stress in soft (a) and hard (b) PZT

The stress-dependent experimental results (Fig. 1) indicate that compressive stress can reduce the apparent internal bias that is caused by the ordered orientation of polar defects. Through the increase in temperature, the influence of stress on the polar defect should increase with the increasing thermally activated mobility of such defects. Soft PZT displays a reduced d_{33} value at 25 °C and a gradual decrease with increasing temperature. Hard PZT, however, clearly shows a two-step switching process with the first decrease occurring at ~40 °C. Importantly for applications, this limits the thermal operating range of such materials when a compressive stress is applied. Above approximately 150 °C, the rate of decrease in d_{33} drops and the subsequent $d_{33}(T)$ behaviour matches well that observed in soft PZT. This two-step switching step is proposed to be due to the reorientation of the polar defects with the application of a bias stress. At lower temperatures, the mobility of the polar defects is low enough that they are not significantly influenced by the stress. However, as the temperature and the mobility increase, they can reorient, which is the origin of the first step. Because they are mechanically clamped, the frequency dispersion at higher temperatures also decreases. Eventually, the material loses the spontaneous polarization and the d_{33} reduces to zero.

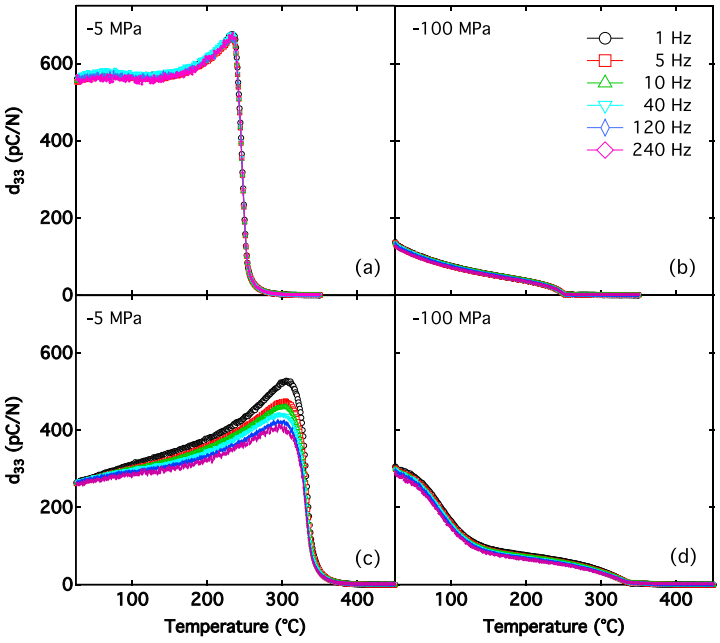

Fig. 2: Temperature-dependent direct piezoelectric coefficient for soft (a), (b) and hard (c), (d) PZT with a bias compressive stress

The present findings indicate that compressive stress reduces the intrinsic forces generated by electrostatic ordering of charged defect population. This resulted in the presence of a two-step switching in hard PZT with increasing temperature that was rationalized to be due to the increasing mobility of the charged point defects, most likely oxygen vacancies. However, further stress-dependent electron paramagnetic resonance measurements are required in order to directly observe stress-induced defect dipole motion.

Nacre forms via Nonclassical and Particle-Mediated Growth Processes

S.E. Wolf

Nature ingeniously designs ceramic materials which serve as sensors, skeletons or armature against predators. Nacre is probably one of the most well studied biominerals. Beside its remarkable and well-known optical properties, its iridescent beauty, this biogenic and self-organized laminate features a hierarchical organization which grants the final biomineral an exceptional toughness. So far, nacre fueled substantially our understanding for structure-property relationships of laminated materials. However, the process by which nacre forms remained for long time enigmatic. In order to gain mechanistical insight into nacre formation, Prof. Dr. S.E. Wolf teamed up with colleagues from Cornell University in order to study the first layer of nacre formed in the bivalve shell of *Pinna nobilis*.

To reach this aim, the research team examined the nacroprismatic transition zone of a large Mediterranean mollusk called the noble pen shell by with high-resolution annular dark-field scanning transmission electron microscopy (ADF-STEM) and selected area electron diffraction (SAED). In order to provide unprecedented large areas of view needed to document the mesoscale self-organization processes occurring at the onset of nacre formation, a novel sample preparation based on a wedge-polishing technique had to be established for biominerals for the first time.

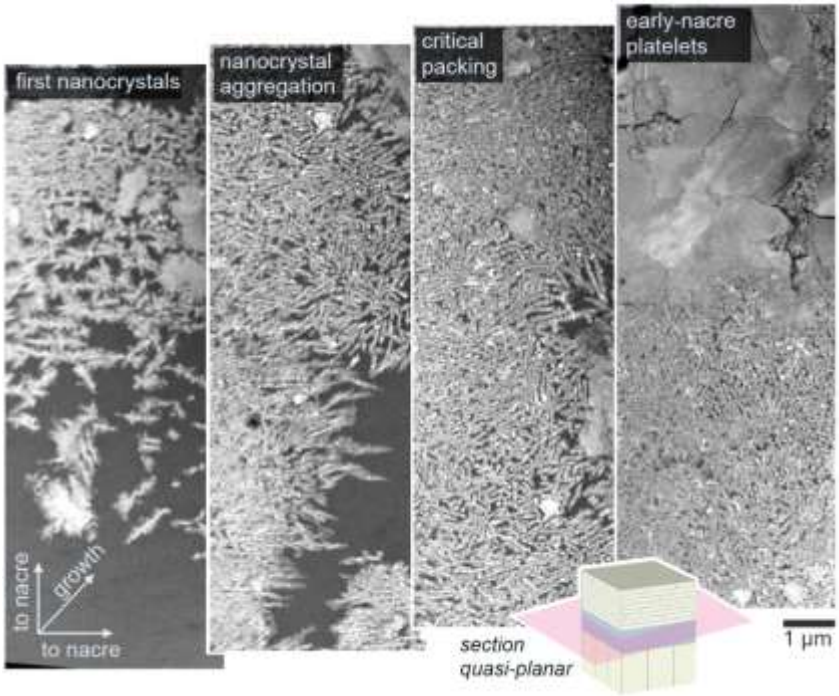

Images with nanometer-scale resolution revealed that the onset of nacre growth occurs from the aggregation of nanoparticles ca. 50–80 nm in size which pack as fiber-like arrangements branching outward with increasing density in the growth direction of the shell. As soon as the particle number density reaches a critical value, the particles merged and formed the first dense and space-filling nacre platelets. The

highly ordered state of nacre is not achieved at once but gradually, transitioning from the densely packed nanofibrillar aragonite, to an early-nacre layer with a higher rate of disorder and tabular waviness until eventually a well-ordered and fully mature nacre is formed.

The cross-section of the nacroprismatic transition zone is a representation, frozen in time, of the transition from one mineralization mechanism to another. It documents clearly that nacre formation occurs by a colloid-mediated growth process and not by an ionic growth process. Therefore, the mineralization of this biogenic and high-performance laminate ceramics follows nonclassical crystallization routes. These findings give new insights into the self-organization mechanisms of nacre and gives new and strong impulses for the generation of biomimetic ceramic materials.

R. Hovden, S.E. Wolf, M.E. Holtz, F. Marin, D.A. Muller, L.A. Estroff
Nanoscale assembly processes revealed in the nacroprismatic transition zone of *Pinna nobilis* mollusc shells
Nature Communication, 2015, 6, 10097, DOI: 10.1038/ncomms10097

c. Publications

Papers

(in alphabetical order)

01/15 **M. Acosta, L.A. Schmitt, L. Molina-Luna, M.C. Scherrer, M. Brilz, K.G. Webber, M. Deluca, H.-J. Kleebe, J. Rödel, W. Donner**
Core-Shell Lead-Free Piezoelectric Ceramics: Current Status and Advanced Characterization of the $Bi_{1/2}Na_{1/2}TiO_3$–$SrTiO_3$ System
Journal of the American Ceramic Society 98 (11) (2015) 3405–3422
DOI: 10.1111/jace.13853

02/15 **M. Beck, K. Hattori, J. Kaschta, K. Kakimoto, A. Roosen**
Lamination and sintering behavior of tape cast, transparent Mg-Al-Spinel ceramics
Ceramics International 41 (3) (2015) 3853-3859
DOI:10.1016/j.ceramint.2014.11.063

03/15 **G.P. Bei, B.J. Pedimonte, M. Pezoldt, J. Ast, T. Fey, M. Goeken, P. Greil**
Crack Healing in $Ti_2Al_{0.5}Sn_{0.5}C$-Al_2O_3 Composites
Journal of the American Ceramic Society 98 (5) (2015) 1604-1610
DOI: 10.1111/jace.13496

04/15 **W. Duan, X. Yin, F. Cao, Y. Jia, Y. Xie, P. Greil, N. Travitzky**
Absorption properties of twinned SiC nanowires reinforced Si_3N_4 composites fabricated by 3D-printing
Materials Letters 159 (2015) 257-260
DOI: 10.1016/j.matlet.2015.06.106

05/15 A.M. Farias, M. Sandrini, J.R.M. Viana, M.L. Baesso, A.C. Bento, J.H. Rohling, Y. Guyot, D. de Ligny, L.A.O. Nunes, F.G. Gandra, J.A. Sampaio, S.M. Lima, L.H.C. Andrade, A.N. Medina

Emission tunability and local environment in europium-doped OH^--free calcium aluminosilicate glasses for artificial lighting applications

Materials Chemistry and Physics 156 (2015) 214-219

DOI: 10.1016/j.matchemphys.2015.03.002

06/15 T. Fey, B. Zierath, P. Greil, M. Potoczek

Microstructural, mechanical and thermal characterization of alumina gel-cast foams manufactured with the use of agarose as gelling agent

Journal of Porous Materials 22 (2015) 1305-1312

DOI: 10.1007/s10934-015-0009-7

07/15 I. Filbert-Demut, G. Bei, T. Höschen, J. Riesch, N. Travitzky, P. Greil

Influence of Ti_3SiC_2 Fiber Coating on Interface and Matrix Cracking in an SiC Fiber-Reinforced Polymer-Derived Ceramic

Advanced Engineering Materials 17 (8) (2015) 1142-1148

DOI: 10.1002/adem.201500192

08/15 I. Filbert-Demut, N. Travitzky, G. Motz, I. Zhitomirsky, P. Greil

Polymer derived ceramics reinforced with Ti_3SiC_2 coated SiC fibers: A feasibility study

Materials Letters 145 (2015) 229–231

DOI: 10.1016/j.matlet.2015.01.128

09/15 Z. Fu, U. Eckstein, A. Dellert, A. Roosen

In situ study of mass loss, shrinkage and stress development during drying of cast colloidal films

Journal of the European Ceramic Society 35 (2015) 2883–2893

DOI: 10.1016/j.jeurceramsoc.2015.03.029

10/15 Z. Fu, P. Polfer, T. Kraft, A. Roosen

Correlation Between Anisotropic Green Microstructure of Spherical-Shaped Alumina Particles and Their Shrinkage Behavior

Journal of the American Ceramic Society 98 (11) (2015) 3438–3444

DOI: 10.1111/jace.13567

11/15 Z. Fu, P. Polfer, T. Kraft, A. Roosen

Three-dimensional shrinkage behavior of green tapes derived from spherical-shaped powders: Experimental studies and numerical simulations

Journal of the European Ceramic Society 35 (8) (2015) 2413–2425

DOI:10.1016/j.jeurceramsoc.2015.01.032

12/15 Z. Fu, A. Roosen

Shrinkage of tape cast products during binder burnout.

J Journal of the American Ceramic Society 98(1) (2015) 20-29

DOI: 10.1111/jace.13270

13/15 R. Gmeiner, U. Deisinger, J. Schönherr, B. Lechner, R. Detsch, A. R. Boccaccini, J. Stampfl

Additive Manufacturing of Bioactive Glasses and Silicate Bioceramics

Journal of Ceramic Science and Technology 6 (2) (2015) 75-86

DOI: 10.4416/JCST2015-00001

14/15 P. Greil

Perspectives of Nano-Carbon Based Engineering Materials

Advanced Engineering Materials 17 (2) (2015) 124–137

DOI: 10.1002/adem.201400110

15/15 J. Harris, I. Mey, M. Hajir, M. Mondeshki, S.E. Wolf

Pseudomorphic transformation of amorphous calcium carbonate films follows spherulitic growth mechanisms and can give rise to crystal lattice tilting

CrystEngComm 17 (2015) 6831-6837

DOI: 10.1039/C5CE00441A

16/15 R. Hovden, S.E. Wolf, M.E. Holtz, F. Marin, D.A. Muller, L.A. Estroff

Nanoscale assembly processes revealed in the nacroprismatic transition zone of Pinna nobilis mollusc shells

Nature Communications 6 (2015) Article number: 10097

DOI: 10.1038/ncomms10097

17/15 Y. Ma, X. Yin, X. Fan, N. Travitzky, P. Greil

Fabrication of MAX-phase-based ceramics by three-dimensional printing

Journal of Ceramic Science and Technology 6 (2) (2015) 87-94

DOI: 10.4416/JCST2015-00006

18/15 Y. Ma, X. Yin, X. Fan, L. Wang, P. Greil, N. Travitzky

Near-net-shape fabrication of Ti_3SiC_2-based ceramics by three-dimensional printing

International Journal of Applied Ceramic Technology 12 (1) (2015) 71-80

DOI:10.1111/ijac.12321

19/15 M.I. Morozov, M.-A. Einarsrud, J.R. Tolchard, P.T. Geiger, K.G. Webber, D. Damjanovic, T. Grande

In-situ structural investigations of ferroelasticity in soft and hard rhombohedral and tetragonal PZT

Journal of Applied Physics 118 (2015) 164104_1-164104_7

DOI: 10.1063/1.4934615

20/15 S.B. Qasim, R.M. Delaine-Smith, T. Fey, A. Rawlinson, I.U. Rehman

Freeze gelated porous membranes for periodontal tissue regeneration

Acta Biomaterialia 23 (2015) 317–328

DOI: 10.1016/j.actbio.2015.05.001

21/15 C.R. Rambo, N. Travitzky, P. Greil

Conductive TiC/Ti-Cu/C composites fabricated by Ti-Cu alloy reactive infiltration into 3D-printed carbon performs

Journal of Composite Materials 49 (16) (2015) 1971-1976

DOI: 10.1177/0021998314541307

22/15 S. Romeis, J. Paul, P. Herre, D. de Ligny, J. Schmidt, W. Peukert

Local densification of a single micron sized silica sphere by uniaxial compression

Scripta Materialia 108 (2015) 84–87

DOI: 10.1016/j.scriptamat.2015.06.023

23/15 J. Schultheiß, B. Dermeik, I. Filbert-Demut, N. Hock, X. Yin, P. Greil, N. Travitzky

Processing and characterization of paper-derived Ti_3SiC_2based ceramic

Ceramics International 41 (10) Part A (2015) 12595-12603

DOI: 10.1016/j.ceramint.2015.06.085

24/15 H. Unterweger, D. Subatzus, R. Tietze1, Ch. Janko, M. Poettler, A. Stiegelschmitt, M. Schuster, C. Maake, A.R. Boccaccini, Ch. Alexiou

International Journal of Nanomedicine 10 (2015) 6985–6996

DOI: 10.2147/IJN.S92336

25/15 M. Vögler, M. Acosta, D.R.J. Brandt, L. Molina-Luna, K.G. Webber

Temperature-dependent R-curve behavior of the lead-free ferroelectric $0.615Ba(Zr_{0.2}Ti_{0.8})O_3–0.385(Ba_{0.7}Ca_{0.3})TiO_3$ ceramic

Engineering Fracture Mechanic 144(2015) 68-77

DOI: 10.1016/j.engfracmech.2015.06.069

26/15 M. Wegener, D. Eckert, A. Roosen

Manufacture of sub-µm thin, particulate-based ITO layers by roller coating

Journal of the European Ceramic Society 35 (8) (2015) 2321–2332

DOI:10.1016/j.jeurceramsoc.2015.02.012

27/15 M. Wegener, M. Kato, K.-I. Kakimoto, S. Spallek, E. Spiecker, A. Roosen

PVP a binder for the manufacture of ultrathin ITO/polymer nanocomposite films with improved electrical conductivity

Journal of Materials Science 50 (18) (2015) 6124-6133

DOI: 10.1007/s10853-015-9168-9

28/15 S.E. Wolf, C. Böhm, J. Harris, M. Hajir, M. Mondeshki, F. Marin

Single nanogranules preserve intracrystalline amorphicity in biominerals

Key Engineering Materials 672 (2015) 47-59

DOI: 10.4028/www.scientific.net/KEM.672.47

29/15 J. Zorzin, E. Maier, S. Harre, T. Fey, R. Belli, U. Lohbauer, A. Petschelt, M. Taschner

Bulk-fill resin composites: Polymerization properties and extended light curing

Dental materials 31 (2015) 293–301

DOI: 10.1016/j.dental.2014.12.010

Volume 17 | Number 36 | 28 September 2015 | Pages 6767–7008

CrystEngComm

www.rsc.org/crystengcomm

Themed issue: Fundamentals of Nanocrystal Formation

ROYAL SOCIETY OF CHEMISTRY

COMMUNICATION
Stephan E. Wolf *et al.*
Pseudomorphic transformation of amorphous calcium carbonate films follows spherulitic growth mechanisms and can give rise to crystal lattice tilting

journal

J. Am. Ceram. Soc., 98 [11] 3405–3422 (2015)
DOI: 10.1111/jace.13853

Core–Shell Lead–Free Piezoelectric Ceramics: Current Status and Advanced Characterization of the $Bi_{1/2}Na_{1/2}TiO_3$–$SrTiO_3$ System

Matias Acosta,[‡] Ljubomira A. Schmitt,[‡] Leopoldo Molina-Luna,[‡] Michael C. Scherrer,[‡] Michael Brilz,[‡] Kyle G. Webber,[‡,§] Marco Deluca,[¶,‖] Hans-Joachim Kleebe,[‡] Jürgen Rödel,[‡] and Wolfgang Donner,[‡,†]

[‡]Department of Materials and Geoscience, Technische Universität Darmstadt, Alarich-Weiss-Straße 2, 64287 Darmstadt, Germany

[§]Department of Materials Science, Friedrich-Alexander-Universität Erlangen-Nürnberg, Martensstraße 5, 91058 Erlangen, Germany

[¶]Materials Center Leoben Forschung GmbH, Roseggerstraße 12, A-8700 Leoben, Austria

[‖]Institut für Struktur- und Funktionskeramik, Montanuniversitaet Leoben, Peter Tunner Straße 5, A-8700 Leoben, Austria

The design of core–shell materials affords additional degrees of freedom to tailor functional properties as compared to solid solution counterparts. Although to date most of the work in core–shell materials has focused on dielectrics, piezoelectric core–shell ceramics may gain similar interest. Generalities of core–shell functional ceramics features are addressed in this work. A model system, $Bi_{1/2}Na_{1/2}TiO_3$–$SrTiO_3$, is introduced to discuss structure–property relationships. We demonstrate that this system features a core–shell microstructure for the composition corresponding to 25 at.% Sr. The material is studied by means of macroscopic functional properties and *in situ* structural characterization techniques at different length scales, such as X-ray diffraction, transmission electron microscopy, and Raman spectroscopy. The evolution of the core–shell with field and temperature determines its functional properties. The high strain of the system, ~0.3% at 4 kV/mm, is due to an electric-field-induced phase transition of the core and shell. Upon field removal the core remains in a poled state, whereas the shell is characterized by a reversible transformation. The reversibility of the phase transition of shells and associated switching are key features in the observed giant strain. Dielectric anomalies are found to be related to changes in oxygen octahedral tilting angles within the core and shell.

I. Introduction

MULTIFUNCTIONAL ceramics are becoming increasingly important in technological devices since they enable coupling between electrical, mechanical, optical, and magnetic properties.[1] Piezoelectrics are technologically relevant due to their ability to transform a mechanical input into an electrical output or vice versa. They are used in a broad variety of devices, such as actuators, motors, sensors, accelerometers, transducers, and acoustic devices, among others.[2–4] For insights into the implementation of piezoelectrics in various actuator devices, the reader is referred to complete overviews given elsewhere.[5–10] The perovskite solid solution family of lead-zirconate-titanate $Pb(Zr,Ti)O_3$ (PZT) is by far the most widely used piezoceramic because of outstanding electromechanical properties that can be tailored to numerous applications through chemical modifications.[11,12]

Global awareness for the environment and sustainability has increased in the past decades.[13] Regulations have been proposed worldwide to minimize the usage of toxic materials in end consumer products. Specifically, Pb and PbO were identified as toxic for human health and the environment.[14] On these grounds, directives against the use of Pb in consumer products have been introduced globally[15–19] leading to the search of lead-free piezoceramics.[12] The interest of piezoelectric device producers to fulfill these regulations and to find new markets is slowly increasing the applicability of lead-free piezoceramics.[20–22] Three main solid solution families have been widely recognized as potential environmentally friendly candidates: $(K,Na)NbO_3$ (KNN)-based, $Bi_{1/2}Na_{1/2}TiO_3$ (BNT)-based, and $BaTiO_3$ (BT)-based materials.[17,22] Lead-free piezoelectrics for small signal applications are at a more mature stage of development than nonresonant large signal piezoelectrics.[22] This entails that to date there is no class of lead-free piezoelectric material that can replace PZT entirely. Research in lead-free piezoceramics has focused mostly in tailoring the electromechanical properties by chemical substitution or microstructure optimization. Recent work, however, has shown the potential of multiphase structures such as ceramic/ceramic composites[23–28] and core–shell materials.[29] This contribution focuses on the

D. Johnson—contributing editor

Manuscript No. 35120. Received December 24, 2014; approved July 20, 2015.
†Author to whom correspondence should be addressed. e-mail: wdonner@ie-darmstadt.de

Feature

Available online at www.sciencedirect.com

ScienceDirect

Ceramics International 41 (2015) 3853–3859

CERAMICS INTERNATIONAL

www.elsevier.com/locate/ceramint

Lamination and sintering behavior of tape cast, transparent Mg–Al–spinel ceramics

M. Beck[a,*], K. Hattori[c], J. Kaschta[b], K. Kakimoto[c], A. Roosen[a]

[a]University of Erlangen-Nuremberg, Department of Materials Science, Glass & Ceramics, Erlangen, Germany
[b]University of Erlangen-Nuremberg, Department of Materials Science, Polymer Materials, Erlangen, Germany
[c]Nagoya Institute of Technology, Institute of Ceramics Research and Education, Nagoya, Japan

Received 29 September 2014; received in revised form 10 November 2014; accepted 11 November 2014
Available online 18 November 2014

Abstract

High purity Mg–Al–spinel powders were processed to form slurries for tape casting. The dried green tapes were cut and laminated via thermo-compression under uniaxial and isostatic pressure conditions. Finally the laminates were sintered pressurelessly in air. The influence of the transformation temperature of the green tape's binder–plasticizer system and of lamination parameters on density and microstructure of the sintered laminates was analyzed. UV-VIS transmission spectroscopy was performed to measure the transparency of the fired laminates. The interrelation between the lamination parameters, sintering behavior and properties of the sintered product is discussed. Isostatic thermal lamination resulted in higher sintered densities than uniaxial lamination. For both techniques an increase in lamination pressure or temperature led to higher relative densities after sintering. The laminates exhibited total forward transmission values of up to 67% at a wavelength of 700 nm.

Keywords: A. Tape casting; D. Spinel; Laminated ceramics; Translucent ceramics

1. Introduction

Transparent ceramics offer a couple of advantageous properties compared to optical glasses. They exhibit higher refractive index values at various Abbé numbers [1,2], an excellent chemical resistance like, e.g., translucent Al_2O_3 in sodium vapor lamps [3], both in combination with mechanical properties which are superior compared to glasses. Besides being a possible candidate as a lens material, Mg–Al–spinel is under intensive research as a material for optical transparent ballistic protection [4–6]. Together with AlON ceramics, spinel seems to be a promising material in this field [7]. Since light is scattered by pores, which leads to a decrease in inline transparency or translucency [8], transparent spinel, as all other transparent polycrystalline materials, has to be processed to a maximum relative density [9]. This is usually achieved by pressure assisted sintering like hot isostatic pressing *HIP* [10,11] and spark plasma sintering *SPS* [12–14].

The goal of this publication is to evaluate tape casting as a possible way of pressureless sintering of transparent or translucent spinel ceramics. This is done by dispersing high purity nanoscaled powders to a minimum agglomerate size. By the addition of binder and plasticizer a ceramic slurry is generated which is de-aired and tape cast to form a thin and flexible green tape after drying [15].

Due to the well dispersed slurries and the resulting homogenous green microstructures, basic requirements are fulfilled for the manufacture of optical transparent ceramics [16,17]. Due to the possibility of lamination, tape casting is also a very flexible process that allows thickness and shape adjustment of substrates. Influences of tape casting and lamination parameters on the density, microstructure and total transmission of spinel are investigated in this paper.

Lamination is usually carried out via thermo-compression [18], in some cases via adhesive tapes [19,20]. During thermo-compression, pressure and temperature are applied to green tapes simultaneously. When the temperature exceeds the glass transition temperature (T_g) of the organic phase within the green tape,

*Corresponding author.
E-mail address: Michael.Beck@ww.uni-erlangen.de (M. Beck).

http://dx.doi.org/10.1016/j.ceramint.2014.11.063
0272-8842/

journal

J. Am. Ceram. Soc., 98 [5] 1604–1610 (2015)
DOI: 10.1111/jace.13496

Crack Healing in $Ti_2Al_{0.5}Sn_{0.5}C$–Al_2O_3 Composites

Guo Ping Bei,[‡,†] Birgit Joana Pedimonte,[‡] Marc Pezoldt,[‡] Johannes Ast,[§] Tobias Fey,[‡] Mathias Goeken,[§] and Peter Greil[‡]

[‡]Department of Materials Science (Glass and Ceramics), University of Erlangen-Nuernberg, Martensstr. 5, Erlangen 91058, Germany

[§]Department of Materials Science (General Material Properties), University of Erlangen-Nuernberg, Martensstr. 5, Erlangen 91058, Germany

Oxidation induced crack healing of Al_2O_3 composites loaded with a MAX phase based repair filler ($Ti_2Al_{0.5}Sn_{0.5}C$) was examined. The fracture strength of 20 vol% repair filler loaded composites containing artificial indent cracks recovered fully to the level of the virgin material upon isothermal annealing in air atmosphere after 48 h at 700°C and 0.5 h at 900°C. SEM-EBSD analysis of crack microstructure indicates two different oxidation reaction regimes to govern the crack filling: near the surface SnO_2, TiO_2, and Al_2O_3 were formed whereas deeply inside the cracks Al_2O_3 and TiO_2 and metallic Sn were detected. The presence of elemental Sn was attributed to partial oxidation of aluminum and titanium which lowered the local oxygen concentration below a threshold value required for Sn oxidation to SnO_2. Thus, $Ti_2Al_{0.5}Sn_{0.5}C$ may represent an efficient repair filler system to trigger oxidation induced crack healing in ceramic composites at temperatures below 1000°C.

I. Introduction

Sintered Al_2O_3 is one of the most important engineering ceramics which is widely being used for numerous wear, chemical, electrical, medical, and other applications. Depending on the residual porosity and purity it may offer high hardness and wear resistance, excellent chemical inertness, high strength, and moderate thermal conductivity as well as good nuclear stability.[1] However, its relatively low fracture toughness <6 $MPam^{1/2}$ may give rise for failure of a mechanically loaded component primarily in the presence of surface cracks. Improving the flaw tolerance envisages toughening of Al_2O_3 by embedding particle or fibers to trigger process zone or crack bridging energy-transfer mechanisms.[2] Another approach is to induce crack healing to recover strength after damage induced crack formation or growth.[3]

Research work on crack healing in Al_2O_3 ceramic can be traced back to 1970s.[4] Gupta *et al.* reported on the crack healing and strength recovery behavior of thermally shocked Al_2O_3 upon annealing above 1400°C.[5] Crack closure was attributed to grain growth and sintering as the dominating mechanisms. Enhanced healing ability was observed when the monolithic Al_2O_3 ceramics were loaded with repair fillers such as SiC particles or whiskers which trigger oxidation crack healing at temperatures below 1400°C.[6,7] Different parameters affecting the healing ability such as annealing temperature and time,[6] crack dimensions,[7] content and characteristics of repair filler,[8,9] healing environment[10] as well as oxygen pressure[11] were investigated. A volume fraction of 15%–20% of SiC repair filler was found to give rise for complete strength recovery of the Al_2O_3/SiC composite.[6,9] Surface cracks of 100–250 μm in length were filled with silica oxidation product after annealing in air at 1300°C for 1 h. Prolonged annealing periods of 10 and 300 h were required when the temperature was reduced to 1200°C and 1000°C,[6] respectively .

More recently, a group of MAX phases $M_{n+1}AX_n$ (n = 1 to 3) where M is a transition metal, A is an A group element, and X is either carbon or nitrogen[12] where shown to exhibit interesting crack healing abilities.[13] For example, in Ti_3AlC_2 extended cracks with a length up to 7 mm and a width of 5 μm could be fully healed after heat treatment at 1100°C for 2 h in air. Superior healing capability observed on Ti_2AlC and Cr_2AlC ceramics was attributed to the formation of adhesive Al_2O_3 filling the space between the disrupted crack surfaces.[14,15] Furthermore, repeatable crack healing was demonstrated on Ti_2AlC.[15] We have reported on the oxidation behavior of $Ti_2Al_{(1-x)}Sn_xC$ MAX phases solid solution.[16] Substitution of Al by Sn was demonstrated to reduce the onset temperature of oxidation from 900°C (Ti_2AlC) down to 700°C (Ti_2SnC). Loading Al_2O_3 with Ti_2SnC repair filler was able to achieve crack healing of the composite at temperatures below 1000°C.[17] The mechanism of crack space filling reaction, however, still remained an open question. Thus, the scope of this work is to investigate the crack filling and strength recovery of Al_2O_3 composite loaded with $Ti_2Al_{0.5}Sn_{0.5}C$ solid solution repair filler. Analyses of the elemental and the phase distribution of the crack filling material were correlated with the recovery kinetics to identify optimized healing conditions.

II. Experimental Procedure

A high purity (> 99.99%) submicrometer alumina powder (AKP-53; Sumitomo Chemical Co., Ltd, Tokyo, Japan) with a mean particle size $d_{0.5)} \approx 0.1$–0.3 μm served as the matrix material for the preparation of the Al_2O_3–MAX phase composites. $Ti_2Al_{0.5}Sn_{0.5}C$ solid solution repair filler with $d_{0.5)} \approx 19$ μm was synthesized from reactant powder mixtures consisting of Ti (4.5 μm, 99.4% purity), Al (<45 μm, 99.5% purity), Sn (2 μm, 99.4% purity) and TiC (2 μm, 99% purity) with a molar composition corresponding to Ti–0.5Sn–0.5Al–0.9TiC and annealed under vacuum at 1400°C for 1 h.

Al_2O_3–$Ti_2Al_{0.5}Sn_{0.5}C$ composites with repair filler fractions of 5, 10, and 20 vol% were sintered at 1350°C for 4 h in Ar atmosphere (Heraeus Holding GmbH, Hanau, Germany) applying a heating rate of 5 K/min. Samples dedicated for mechanical investigation were polished to 1 μm surface finish with diamond suspension and cut into bar specimens with dimensions of 2.5 mm^3 × 2.0 mm^3 × 27 mm^3. Surface cracks were generated by means of Vickers' indentation

F. Wakai—contributing editor

Manuscript No. 35832. Received October 27, 2014; revised January 8, 2015; approved January 8, 2015.
†Author to whom correspondence should be addressed. e-mail: guoping.bei@ww.uni-erlangen.de

Materials Letters 159 (2015) 257–260

Contents lists available at ScienceDirect

Materials Letters

journal homepage: www.elsevier.com/locate/matlet

Absorption properties of twinned SiC nanowires reinforced Si_3N_4 composites fabricated by 3D-prining

Wenyan Duan [a], Xiaowei Yin [a,*], Fangxian Cao [a], Yinglu Jia [a], Yun Xie [a], Peter Greil [b], Nahum Travitzky [b,**]

[a] Science and Technology on Thermostructural Composite Materials Laboratory, Northwestern Polytechnical University, Xi'an 710072, China
[b] Department of Materials Science, Institute of Glass and Ceramics, University of Erlangen-Nuremberg, Martensstr. 5, d-91058 Erlangen, Germany

ARTICLE INFO

Article history:
Received 17 February 2015
Received in revised form
22 May 2015
Accepted 28 June 2015
Available online 4 July 2015

Keywords:
Si_3N_4–SiC
3D-printing
PIP
Absorption properties

ABSTRACT

Near net- and complex shaped porous silicon nitride (Si_3N_4) composites reinforced with in-situ formed twinned silicon carbide (SiC) nanowires (NWs) were successfully fabricated by 3D-printing (3DP) followed by polymer precursor infiltration and pyrolysis (PIP) up to 1400 °C. An increase of the PIP cycle number of the printed bodies resulted in a homogeneous distribution of SiC NWs in the fabricated composites. An increase of SiC NW content in the fabricated composites led to the growth of both the real and the imaginary parts of permittivity. The formation of twinned SiC NWs with high electrical conductivity led to a minimal electromagnetic wave RC of −57 dB, demonstrating that Si_3N_4–SiC ceramics with the in-situ formed SiC NWs have a superior microwave absorbing ability.

1. Introduction

Recent years, many research works have been carried out to investigate the microwave absorption properties of different materials [1–3] for protecting environment and sensitive circuits from microwave radiation. When the reflection coefficient (RC) of an electromagnetic wave (EMW) absorbing material is smaller than −10 dB, only 10% of EMW power is reflected and 90% is absorbed. Silicon based ternary polymer-derived ceramics (PDC) have attracted attention for their EMW absorbing properties and stability with respect to crystallization and decomposition, and oxidation [4]. Table 1 shows EMW absorbing properties of PDCs [5–9], which can be easily tailored. The RC of PDCs can be lowered to less than −10 dB. In order to obtain improved EMW absorption property, absorbing materials need to have a promising permittivity [10]. At a frequency of 10 GHz and a sample thickness of 2.86 mm, the optimum ε' and ε'' should be equal to 7.3 and 3.3 to get the minimum RC [11]. However, the permittivity of the already-reported PDCs deviated from this optimizing permittivity.

To optimize permittivity, EMW absorption materials should contain part of the following components: nano-sized pores, nano-sized secondary phase, conductive/semi-conductive secondary phase and insulating matrix [10]. Porous silicon nitride (Si_3N_4) was selected as the insulating matrix for its excellent mechanical properties and promising EMW transparent properties. Porous Si_3N_4 can be fabricated by nitriding silicon powder compacts in the temperature range 1100–1450 °C [12]. Owing to the inability of current technology to produce complex-shaped ceramic, 3D-printing (3DP) is becoming an increasingly important processing technique. For instance, Fig. 1a and b show the computer-aided design model and the Si_3N_4 printed part. 3DP enables user to fabricate such complex-shaped components with high reliability. By applying 3DP it is possible to design materials with moderate micro and nano-sized porosity which can be post-infiltrated with conductive/semi-conductive secondary phase.

SiC is a wide band gap semiconductor which has many practical applications in EMW absorption [13]. PDC-SiC nanowires (NWs) have higher electrical conductivity than grained SiC due to the special structure of one dimensional NW on a nanometer scale [14]. EMW absorption property of Si_3N_4–SiC can be substantially increased for the formation of PDC-SiC NWs in the porous Si_3N_4 ceramic by precursor infiltration and pyrolysis (PIP). It is important to note that in-situ forming of SiC NWs may avoid health hazards associated with fine ceramic reinforcement.

In this work, the combination of 3DP and PIP was for the first time employed to fabricate Si_3N_4–SiC composites. This approach enables the near net-shape fabrication, microstructure designing and improvement of absorption property. The effects of SiC NWs on the microstructure, dielectric properties, and absorption

* Corresponding author. Fax: +86 29 88494620.
** Corresponding author. Fax: +49 9131 852 8311.
E-mail addresses: yinxw@nwpu.edu.cn (X. Yin), nahum.travitzky@ww.uni-erlangen.de (N. Travitzky).

http://dx.doi.org/10.1016/j.matlet.2015.06.106
0167-577X/

Materials Chemistry and Physics 156 (2015) 214–219

Contents lists available at ScienceDirect

Materials Chemistry and Physics

journal homepage: www.elsevier.com/locate/matchemphys

Emission tunability and local environment in europium-doped OH^--free calcium aluminosilicate glasses for artificial lighting applications

Aline M. Farias [a], Marcelo Sandrini [a], José Renato M. Viana [a], Mauro L. Baesso [a], Antônio C. Bento [a], Jurandir H. Rohling [a], Yannick Guyot [b], Dominique De Ligny [c], Luiz Antônio O. Nunes [d], Flávio G. Gandra [e], Juraci A. Sampaio [f], Sandro M. Lima [g], Luis Humberto C. Andrade [g], Antônio N. Medina [a, *]

[a] Departamento de Física, Universidade Estadual de Maringá, Av Colombo, 5790, 87020-900, Maringá, PR, Brazil
[b] Laboratoire de Physico–Chimie des Matériaux Luminescents, Université de Lyon, Université Claude Bernard Lyon 1, Villeurbanne, UMR 5620 CNRS 69622, France
[c] Department of Materials Science and Engineering, University of Erlangen Nürnberg, Martens str. 5, 91058, Erlangen, Germany
[d] Instituto de Física de São Carlos, Universidade de São Paulo, Av. Trabalhador São-Carlense400, 13566-590, São Carlos, SP, Brazil
[e] Instituto de Física Gleb Wataghin, Universidade Estadual de Campinas, 13083-859, Campinas, SP, Brazil
[f] Lab Ciências Físicas, Universidade Estadual Norte Fluminense, 28013-602, Campos Dos Goytacazes, RJ, Brazil
[g] Grupo de Espectroscopia Óptica e Fototérmica, Universidade Estadual de Mato Grosso do Sul-UEMS, Dourados, MS, C. P. 351, CEP 79804-970, Brazil

HIGHLIGHTS

- Eu^{2+}-doped OH^- free calcium aluminosilicate glass as a new source for white lighting.
- Correlation between emission tunability and local environment of europium ions.
- Significant reduction of Eu^{3+} to Eu^{2+} by melting the glasses under vacuum atmosphere.
- Broad, intense and tunable luminescence ranging from blue to red.

ARTICLE INFO

Article history:
Received 24 July 2014
Received in revised form
23 February 2015
Accepted 1 March 2015
Available online 9 March 2015

Keywords:
Glasses
Luminescence
Optical properties
XAFS (EXAFS and XANES)
Photoluminescence spectroscopy
Visible and ultraviolet spectrometers

ABSTRACT

The relationship between emission tunability and the local environment of europium ions in OH^--free calcium aluminosilicate glasses was investigated, focusing on the development of devices for artificial lighting. Significant conversion of Eu^{3+} to Eu^{2+} was obtained by means of melting the glasses under a vacuum atmosphere and controlling the silica content, resulting in broad, intense, and tunable luminescence ranging from blue to red. Electron spin resonance and X-ray absorption near edge structure measurements enabled correlation of the luminescence behavior of the material with the Eu^{2+}/Eu^{3+} concentration ratio and changes in the surrounding ions' crystal field. The coordinates of the CIE 1931 chromaticity diagram were calculated from the spectra, and the contour maps showed that the light emitted from Eu^{2+} presented broad bands and enhanced color tuning, ranging from reddish-orange to blue. The results showed that these Eu doped glasses can be used for tunable white lighting by combining matrix composition and the adjustment of the pumping wavelength.

1. Introduction

A major challenge in the development of a new generation of artificial lighting is the tailoring of phosphor materials that possess efficient and tunable emissions across the whole range of the visible spectrum [1–7]. Europium and cerium are currently the most widely used phosphors in devices for lighting and displays, and both can coexist in several oxidation states in the host matrices. In addition, their emissions are known to be strongly dependent on the surrounding ions' crystal field [2].

* Corresponding author.
E-mail address: medina@dfi.uem.br (A.N. Medina).

http://dx.doi.org/10.1016/j.matchemphys.2015.03.002
0254-0584/

J Porous Mater (2015) 22:1305–1312
DOI 10.1007/s10934-015-0009-7

Microstructural, mechanical and thermal characterization of alumina gel-cast foams manufactured with the use of agarose as gelling agent

Tobias Fey[1] · Bodo Zierath[1] · Peter Greil[1] · Marek Potoczek[2]

Published online: 30 June 2015

Abstract Alumina gel-cast foams manufactured by using agarose as gelling agent were examined in terms of microstructural, mechanical and thermal properties. The microstructural SEM measurements of alumina foams were compared with X-ray micro tomography investigations also on the pore network. Young's modulus of alumina foams was determined by impulse excitation and ultrasonic sound velocity measurements. These two independent techniques showed similar results. Gibson and Ashby's model of completely open-cell and closed-cell foams was compared with experimental data from compression tests. The thermal conductivity measurements using laser-flash analysis were correlated with the pore network in the alumina foam structure.

Keywords Gel-cast foams · Agarose · Alumina · Micro-CT · Porous ceramics · Thermal conductivity · Mechanical properties · Pore network

1 Introduction

Cellular ceramics are very attractive for a wide range of applications [1, 2] due to their high porosity, high gas permeability, good mechanical stiffness, and good thermal shock resistance. In recent years, a new class of ceramic foams with porosity levels up to 90 % had been developed by combining the gel-casting process and the aeration of the ceramic suspension containing foaming agents and gelling agents [3, 4]. These foams exhibit a high interconnected porous network of spherical cells interconnected by circular windows. The main disadvantages of the conventional gel-casting processes for dense components and foams is the neurotoxicity acrylamide. For this reason processes of reduced toxicity were developed. Many alternative gelling systems for the gel-casting of foams based on low-toxicity monomers were demonstrated by Ortega et al. [5] and a low toxic epoxy resin system was demonstrated by Mao et al. [6]. Gel-casting techniques utilizing environmentally friendly biopolymers as gel-formers in manufacturing of ceramic foams were intensively studied: different biopolymers such as gelatin [6], proteins (ovalbumine and bovine serum albumin) [7–10], sucrose [11], agar [12], starch [13], and wheat particles [14] have recently been applied as non-toxic components for the fabrication of gel-cast ceramic foams.

However, the change of gelling conditions by changing the gelling agent may influence the microstructure of gel-cast ceramic foams, as cell diameter, interconnected windows size, strut thickness and therefore their mechanical properties. In general the cell size, windows size, and strut thickness depend on the foam destabilization processes occurring during the time interval between foaming and gelation. For this reason the influence of gelling binder on microstructural and mechanical properties of ceramic foams should be intensively studied.

In this work we have studied the microstructural, mechanical and thermal properties of alumina foams manufacturing by the use of agarose as gelling agent. Agarose and agar belong to polysaccharides which are formed as a result of transitions hydrogels of a double helix. These environmentally friendly polysaccharides

✉ Tobias Fey
tobias.fey@fau.de

[1] Department of Material Science, University Erlangen-Nürnberg, Martensstr. 5, 91058 Erlangen, Germany

[2] Faculty of Chemistry, Rzeszow University of Technology, Powstancow Warszawy Ave. 12, 35-959 Rzeszow, Poland

FULL PAPER

ADVANCED ENGINEERING MATERIALS

DOI: 10.1002/adem.201500192

Influence of Ti_3SiC_2 Fiber Coating on Interface and Matrix Cracking in an SiC Fiber-Reinforced Polymer-Derived Ceramic**

By *Ina Filbert-Demut,* Guoping Bei, Till Höschen, Johann Riesch, Nahum Travitzky* and Peter Greil*

The effect of Ti_3SiC_2 coatings on the interfacial properties of SiC-fiber reinforced FeSiCr/SiC-filled polymethylsilsesquioxane-derived ceramics was investigated. An electrophoretically deposited Ti_3SiC_2 coating was prepared on the fiber/matrix interface. Interfacial parameters such as frictional sliding stress and fracture energy were derived from fiber push-out tests and correlated to the thickness of the Ti_3SiC_2 layer. Compared to uncoated fibers, the Ti_3SiC_2 interlayer gives rise for a pronounced enhance of interface shear strength, coefficient of friction, and sliding strength but a reduced fracture energy. With increasing Ti_3SiC_2 coating thickness, thermal mismatch-induced residual compressive stresses at the fiber/matrix interface tend to decrease significantly.

1. Introduction

Fracture behavior of continuous fiber-reinforced ceramic matrix composites is substantially dominated by the fiber/matrix interface characteristics. Generally, a weak fiber-matrix bonding encourages interface debonding and fiber sliding, which promotes bridging of matrix cracks by fiber pull-out.[1] The bonding strength can be properly controlled by deposition of a fiber coating prior to incorporation into matrix. Appropriate coatings should be thermochemical and thermomechanical compatible with the fiber and the matrix constituents and provide acceptable values of interfacial shear strength and frictional sliding resistance. Materials such as pyrocarbon (PyC) and hexagonal boron nitride (h-BN) were extensively explored as interlayer in fiber-reinforced non-oxide ceramic matrix composites (CMCs).[2–6] Although their effectiveness is undoubtedly confirmed, these interlayers suffer from low oxidation resistance at elevated temperatures.

MAX phases are layered ternary compounds $M_{n+1}AX_n$, where n is 1–3, M is an early transition metal, A is an element of the A-group (mostly IIIA and IVA), and X is carbon (C) or nitrogen (N). Their crystal structure can be described as close-packed layers of A-group elements periodically intercalated into $M_{n+1}X_n$ polyhedral layers with X located in the center of a polyhedral which are arranged to edge-bonded planar layers.[7] The rather weak bonding between the A-layers and the $M_{n+1}X_n$ layers is accountable for the significant anisotropy of thermal expansion,[8] Young's modulus,[9] and hardness.[10] The layered microstructure favors an unusual deformation capability involving delamination and formation of kink bands within the basal planes, resulting in an outstanding damage tolerance.[10,11] In addition, their excellent thermal shock[12] and inherent oxidation resistance[13] render them attractive for the use as interfacial coatings. Furthermore, the wide variation of MAX phase composition with more than 50 phases reported in the literature[14] can be used to tailor the mechanical and thermal properties of an interface layer in order to optimize fiber/matrix bonding in a composite in this work. Ti_3SiC_2 layers were electrophoretically deposited on continuous SiC fibers prior to incorporation into a polymer-derived ceramic (PDC) matrix.[15] The conversion of filler-loaded organometallic precursors into ceramics has been noted as one of the most promising techniques of fabrication of dense polymer-derived ceramic composites due to volume reactions during the ceramization of the polymer.[16,17]

[*] *I. Filbert-Demut, Dr. G. Bei, PD Dr. N. Travitzky, Prof. P. Greil*
Department of Material Science, Glass and Ceramics, University of Erlangen-Nuremberg, Martensstr. 5 91058, Erlangen, Germany
E-mail: ina.filbert@fau.de; nahum.travitzky@fau.de
T. Höschen, Dr. J. Riesch
Max-Planck-Institut für Plasmaphysik, Boltzmannstr. 2, 85748, Garching, Germany

[**] *The authors are grateful for the financial support of the German Research Foundation graduate school 1229 "Stable and metastable multiphase systems at high application temperatures".*

Materials Letters 145 (2015) 229–231

Contents lists available at ScienceDirect

Materials Letters

journal homepage: www.elsevier.com/locate/matlet

Polymer derived ceramics reinforced with Ti_3SiC_2 coated SiC fibers: A feasibility study

Ina Filbert-Demut [a,*], Nahum Travitzky [a,*], Günter Motz [b], Igor Zhitomirsky [c], Peter Greil [a]

[a] Department of Material Science, Glass and Ceramics, Friedrich-Alexander-Universität Erlangen-Nuremberg, Martensstr. 5, 91058 Erlangen, Germany
[b] Ceramic Materials Engineering, University of Bayreuth, Ludwig-Thoma-Str. 36b, 95440 Bayreuth, Germany
[c] Department of Material Science and Engineering, McMaster University, 1280 Main Street West, Hamilton, Ontario, Canada L8S 4L7

ARTICLE INFO

Article history:
Received 10 November 2014
Accepted 24 January 2015
Available online 3 February 2015

Keywords:
Ti_3SiC_2
Electrophoretic deposition
Interlayer
Polymer derived ceramics
Fiber-reinforced composites

ABSTRACT

Owing to the remarkable mechanical and thermal properties of MAX-phases, Ti_3SiC_2 was explored as an interlayer material for fiber-reinforced ceramic composites. Electrophoretic deposition was applied to prepare Ti_3SiC_2 coatings on SiC monofilaments with coating thickness ranging from 400 nm to 400 μm. High deposition rate and suspension stability were achieved using a polyelectrolyte dispersant. The dispersant amount was optimized by zeta potential and viscosity measurements. The coated SiC fibers were incorporated by uniaxial warm-pressing in a FeSiCr/SiC-loaded polymethylsilsesquioxane (PMS) matrix. After pyrolysis at 1200 °C in Argon a dense material was obtained.

1. Introduction

The development of ceramic composites with high structural reliability and long-term durability is a subject of intensive research. Toughening of brittle ceramic matrix may be achieved by incorporation of reinforcing elements, such as high strength fibers, which trigger enhanced crack bridging and fiber-pull-out [1]. The fiber/matrix interface plays a key role in controlling load transfer from the matrix to the fiber. One of the important engineering challenges is the design of the fiber/matrix interfacial coatings, which can reduce residual stresses by tailoring the shear strain behavior [2].

Nanolaminates with a layered $M_{n+1}AX_n$ crystal structure (so called MAX-phases with $n=1$–3, M: early transition metal, A: A group element, X: C or N) exhibit a remarkable combination of properties, making them attractive for the application in interfacial coatings [3]. For example, Ti_3SiC_2 with excellent mechanical properties such as flexural strength of 450 MPa [4] and Young's modulus of 322 GPa [5] demonstrated superior damage tolerance by delamination and kink-band formation [6], outstanding thermal shock behavior [7] and capability to withstand oxidation and hot corrosion up to 1100 °C by formation of protective titania and silica scales [8].

Electrophoretic deposition (EPD) [9,10] was selected as a promising method for the fabrication of uniform Ti_3SiC_2 coatings of controlled thickness on substrates of complex shape. The feasibility to coat individual fibers, 2-D and 3-D fibrous substrates by EPD with various materials has been successfully demonstrated [11–14]. Recently EPD was applied for the fabrication of Ti_3SiC_2 coatings on conductive substrates [15–17]. In these cases, the investigations were mostly focused on the analysis of the deposition kinetics and film formation mechanisms.

One of the most promising cost-effective techniques for the fabrication of ceramic matrices is the polymer derived ceramics (PDCs) route, where the addition of fillers may considerably reduce the volume shrinkage of the polymer precursor associated with the thermal-induced conversion into ceramics [18].

It was the aim of the present work to coat continuous SiC fibers with a Ti_3SiC_2 layer and to incorporate them into ferrosilicochromium (FeSiCr)- and SiC-loaded polymethylsilsesquioxane matrix and thus, to demonstrate the feasibility for the fabrication of MAX-phase coated fibers reinforced PDCs.

2. Experimental procedure

Ti_3SiC_2 powder (Beijing Jinhezhi Material Co., China, $d_{50}=12$ μm) was dispersed in ethanol in an agitator bead mil for 4 h at 1500 rpm. The mill was equipped with a coolable grinding tank and filled with ZrO_2 grinding beads with a diameter of 0.2–0.3 mm. The particle size and the specific surface area of the milled powders were determined by laser scattering and gas adsorption, respectively. The used silicon carbide fibers (SCS-6, Specialty Materials Inc., USA) have a diameter of 142 μm and an outermost carbonaceous coating with thickness of approximately 3 μm.

* Corresponding authors. Tel.: +49 9131 85 28561, +49 9131 85 28775.
E-mail addresses: ina.filbert@fau.de (I. Filbert-Demut), nahum.travitzky@fau.de (N. Travitzky).

http://dx.doi.org/10.1016/j.matlet.2015.01.128
0167-577X/

Available online at www.sciencedirect.com
ScienceDirect
Journal of the European Ceramic Society 35 (2015) 2883–2893
www.elsevier.com/locate/jeurceramsoc

In situ study of mass loss, shrinkage and stress development during drying of cast colloidal films

Zongwen Fu, Udo Eckstein, Armin Dellert, Andreas Roosen *

University of Erlangen-Nuremberg, Department of Materials Science, Glass and Ceramics, Martensstrasse 5, 91058 Erlangen, Germany

Received 13 January 2015; received in revised form 13 March 2015; accepted 21 March 2015
Available online 11 April 2015

Abstract

During constrained drying of binder-assisted colloidal coatings on rigid substrates, drying stress-induced defects such as cracks and warpage can often be observed due to the lateral confinement of the film by the substrate. The purpose of the current work is to understand the origin of these drying defects and to develop strategies for their avoidance by the adjustment of slurry composition or processing parameters. In this paper, the time-dependent drying behavior of colloidal ceramic coatings was studied in situ by observation of mass loss, drying shrinkage and drying stress by different methods, such as transparent substrate deflection and beam deflection methods. The stress development and the critical moment, at which cracks form, were investigated in films of different compositions with respect to solvent, particle size, binder and plasticizer. The origins of the measured differences in drying shrinkage, crack formation as well as residual stresses after drying were discussed.

Keywords: Tape casting; Drying stress; Drying shrinkage; Drying cracks; In situ measurement

1. Introduction

Tape casting is widely used for manufacturing thin ceramic sheets in a thickness range between 10 and 1000 μm for various applications, e.g. capacitors, sensors and high integrated circuits [1–3]. The principle of this wet ceramic forming process is based on the deposition of a colloidal suspension, which is commonly composed of solvent, ceramic powder, dispersion agent and organic additives, like binder, plasticizer, defoamer, on a moving carrier film by means of the doctor blade technique [1,4]. The drying of the deposited layer plays a critical role in the whole process chain. During drying, the solvent is removed from the colloidal system [5], which causes a pronounced drying shrinkage; due to the adhesion of the cast film on the substrate this drying shrinkage only occurs in the thickness direction [1]. This constrained and therefore inhomogeneous drying process can cause stresses and defects such as warpage and cracks [6]. After drying, a flexible porous green tape is obtained. During storage of tape cast green sheets, aging effects, e.g. shrinkage of green tapes at room temperature, can often be observed due to stress relaxation of the polymer matrix after drying [7].

Therefore, one of the main challenges associated with the tape casting technique is to understand the origin of drying defects and residual stresses as well as drying stress development. To measure the drying stress, several techniques have been developed [5,6,8–11]. Bauer et al. [5] used the transparent substrate deflection method to determine the drying stress in aqueous slurries; at the same time, in situ observation of the drying front was also possible. Raju et al. [9] and Lewis et al. [4,12,13] investigated stress development during drying by means of the photoelasticity method and cantilever deflection method, respectively. The drying stress indicated the propensity of crack formation as a consequence of the capillary pressure in ceramic coatings; each sudden drop in the drying stress curve indicated formation of a crack [6]. Furthermore, it was found that during drying due to the transport of solvent from the bottom to the upper side, an increased amount of the dissolved binder was observed at the top surface of the tape [14]. This gradient distribution of particles and binder, respectively, resulted in a different drying shrinkage between the top and bottom of the tape which led to the concave bending of the film on the substrate; resulting in a bent film which was stressed in lateral

* Corresponding author. Tel.: +49 9131 8527547; fax: +49 9131 8528311.
E-mail address: andreas.roosen@fau.de (A. Roosen).

http://dx.doi.org/10.1016/j.jeurceramsoc.2015.03.029
0955-2219/

J. Am. Ceram. Soc., 98 [11] 3438–3444 (2015)
DOI: 10.1111/jace.13567

journal

Correlation Between Anisotropic Green Microstructure of Spherical-Shaped Alumina Particles and Their Shrinkage Behavior

Zongwen Fu,[‡] Pit Polfer,[§] Torsten Kraft,[§] and Andreas Roosen[‡,¶]

[‡]Department of Materials Science, Glass and Ceramics, University of Erlangen-Nuremberg, Martensstrasse 5, Erlangen 91058, Germany

[§]Fraunhofer-Institute for Mechanics of Materials IWM, Wöhlerstrasse 11, Freiburg 79108, Germany

Dimensional control is one of the basic problems in ceramic processing, especially for tape cast ceramic sheets which are used to build up multilayer structures for high-integrated components. Uncontrolled anisotropic shrinkage can cause geometrical distortion and circuit failure of multilayer ceramics during sintering. The understanding of the relationship between green tape microstructure and shrinkage anisotropy is of great importance for further miniaturization of multilayer devices. In this study, alumina powders with spherical particle shape were used to cast green tapes. The microstructure as well as the pore orientation and the shrinkage behavior were analyzed. According to the sintering theory, grain growth and pore elimination are the two most important mechanisms to describe sintering shrinkage. In this work, three-dimensional shrinkage behavior of tape cast alumina powders with spherical particle shape was investigated and correlated with pore orientation in the microstructure. Specifically, the reason for the different shrinkage in *z*-direction compared to the lateral shrinkage is in focus. The study is based on experiments as well as on mathematical visualization.

I. Introduction

During sintering of tape cast products, which require high dimensional accuracy for the use of high-integrated components, an anisotropic shrinkage can be observed,[1–4] which is attributed to an anisotropic green microstructure. During tape casting, nonspherical particles are oriented caused by shearing and constrained drying[5–7] resulting in a higher sintering shrinkage in the thickness direction than in the lateral direction. However, samples composed of spherical particles also exhibit anisotropic shrinkage behavior during sintering.[8,9] In this study, tapes composed of almost spherical particles were investigated experimentally and analytically. To achieve a better understanding for the reason of the higher shrinkage in the *z*-direction compared to the lateral shrinkage, the shrinkage behavior was analyzed after binder removal and sintering at different temperatures in all three spatial directions. The correlation between anisotropic shrinkage and microstructure of the green tape concerning pore orientation was discussed.

D. Bouvard—contributing editor

Manuscript No. 36075. Received December 15, 2014; approved February 17, 2015.
[¶]Author to whom correspondence should be addressed.
e-mail: andreas.roosen@fau.de

II. Experimental Procedure

(1) Slurry Preparation, Tape Casting, and Thermal Treatment

A nearly spherical alumina powder SP (d_{50}: ~3 μm; Sumitomo Chemical Co., Ltd., Tokyo, Japan) with a narrow Gaussian shaped particle size distribution (d_{10}: ~2 μm, d_{90}: ~8 μm) was used in this study.

Table I shows the exact composition of the tape casting slurry used in this study and also the density of the components. The slurry was based on organic solvents containing 68 mass% ethanol and 32 mass% toluene. The solid loading of SP-powder in the slurry was kept at 28 vol%. Menhaden Fish oil (Kellogg Co., Buffalo, NY), polyvinyl butyral (B-98; Solutia Inc., St. Louis, MO) and alkyl benzyl phthalate (Santicizer S261A; Ferro Corp., Cleveland, OH) were used as dispersant, binder, and plasticizer, respectively. The slurry preparation and tape casting process were described in detail by Fu *et al.*[8] A silicon-coated PET film (Mitsubishi Plastics, Inc., Tokyo, Japan) with a thickness of ~100 μm was used as tape carrier. To obtain tapes with a homogenous tape thickness, a tape casting machine with a fixed double chamber casting head was used maintaining an invariable low hydrostatic pressure.[10] The front and rear doctor blades were adjusted to a gap height of 900 and 1100 μm, respectively, resulting in dried tapes with a thickness of 250 ± 10 μm. According to Watanabe *et al.*[11] increasing shear rates above ~12.5 s^{-1} does not result in an increased particle orientation degree, thus the casting speed was set to 700 mm/min, resulting in a shear rate of ~13.0 s^{-1}. At this shear rate the slurry exhibits a viscosity of 3.7 Pa·s.

The dried green tapes were removed from the PET carrier tape and cut to the desired sample dimension with a hot knife (Groz-Beckert KG, Albstadt, Germany) at 60°C. The samples were then placed on smooth, high-purity alumina setters (Kerafol GmbH, Eschenbach, Germany) for binder burnout (BBO). Debinding took place in air with a heating rate of 2 K/min up to 450°C for 1 h, followed by prefiring at 1600°C with a holding time of 1 h and a heating rate of 4 K/min. At this temperature the SP-powder exhibits a linear shrinkage less than 4%, which is sufficient to determine the anisotropy of shrinkage, but low enough to preserve the microstructure of the green tape for characterization; prefiring also gives the tape sufficient strength for the preparation of cross sections. To improve the densification, the prefired tapes were subsequently sintered at 1600°C for 10 h as well as at 1730°C for 5 h and for 15 h, respectively. To ensure free sintering the setters used during thermal treatments from 1600°C to 1730°C were coated with a thin layer of Al_2O_3 parting sand with a mean particle size of 150 μm. The theoretical density of ceramic tapes before and after firing was calculated using the theoretical density values shown in Table I. The bulk density of green tapes was determined by measuring the weight, the area by scanning the

Available online at www.sciencedirect.com
ScienceDirect
Journal of the European Ceramic Society 35 (2015) 2413–2425
www.elsevier.com/locate/jeurceramsoc

Three-dimensional shrinkage behavior of green tapes derived from spherical-shaped powders: Experimental studies and numerical simulations

Zongwen Fu [a], Pit Polfer [b], Torsten Kraft [b], Andreas Roosen [a,*]

[a] University of Erlangen-Nuremberg, Department of Materials Science, Glass and Ceramics, Martensstrasse 5, 91058 Erlangen, Germany
[b] Fraunhofer Institute for Mechanics of Materials IWM, Wöhlerstrasse 11, 79108 Freiburg, Germany

Received 13 August 2014; received in revised form 22 January 2015; accepted 30 January 2015
Available online 20 February 2015

Abstract

In tape-cast products a higher shrinkage is observed in the thickness direction compared to the in-plane shrinkage, which is attributed to an anisotropic green tape microstructure caused by shearing and drying during manufacturing. In the present study, cast tapes composed of spherical particles were investigated experimentally and numerically. The shrinkage behavior was analyzed after binder removal and sintering at different temperatures in all three spatial directions. The correlation between anisotropic shrinkage and microstructure concerning pore orientation and coordination number was discussed. Furthermore, it is shown that the anisotropic shrinkage during binder removal contributes strongly to the total shrinkage anisotropy.

Keywords: Tape casting; Anisotropic shrinkage; Ceramic sintering; Discrete element method; Simulation

1. Introduction

Dimensional control is one of the basic problems in ceramic processing, especially for tape cast sheets which are used to manufacture multilayer structures with highly integrated components.[1,2] In this technology, the exact positions, e.g., of vias or electrodes in different layers must be maintained during the entire thermal process.[2] Therefore, any uncontrolled shrinkage anisotropy during binder burnout and sintering can lead to device failure.[3–6] During tape casting, due to the shear flow gradient under the blade of the casting head as well as to the constrained drying process, non-spherical ceramic particles are predominantly oriented parallel to the casting direction.[7–15] Because of this anisotropic green tape microstructure, anisotropic shrinkage occurs:[8,13,14,16]

$$\varepsilon_z \gg \varepsilon_y \gg \varepsilon_x \quad (1)$$

where ε represents the linear sintering shrinkage and x, y and z denote the casting, transverse and thickness direction, respectively.

Not only tape-cast products exhibit an anisotropic microstructure; the shrinkage anisotropy could also be observed during the sintering of uniaxially pressed, extruded and three-dimensional printed ceramics.[17–19] During uniaxial pressing, extrusion and tape casting, it was found that non-spherical ceramic particles can be textured and that the largest and smallest shrinkages occur in the directions perpendicular and parallel to the particle orientation direction, respectively.[17] During rapid prototyping based on layer-by-layer assemblies via 3D printing, elongated pores perpendicular to the thickness direction as well as a layered microstructure could be found.[18,19] In all these cases a higher shrinkage in the z-direction was observed; the primary cause of anisotropic shrinkage in these systems is attributed to the orientation of anisotropic particles.[11,16,19–25] Wakai et al. simulated the shrinkage behavior of spherical particles, which are not oriented but which also exhibit anisotropic shrinkage behavior caused by particle rearrangement during sintering due to an inhomogeneous distribution of contact points.[26]

* Corresponding author. Tel.: +49 91318527540.
E-mail address: andreas.roosen@fau.de (A. Roosen).

http://dx.doi.org/10.1016/j.jeurceramsoc.2015.01.032
0955-2219/

journal

J. Am. Ceram. Soc., 98 [1] 20–29 (2015)
DOI: 10.1111/jace.13270

Shrinkage of Tape Cast Products During Binder Burnout

Zongwen Fu and Andreas Roosen†

Department of Materials Science, Glass and Ceramics, University of Erlangen-Nuremberg, Martensstrasse 5, Erlangen 91058, Germany

During sintering of tape cast products, anisotropic shrinkage occurs, which can be attributed to an anisotropic green tape structure concerning particle and pore orientation. Little is known about the shrinkage during binder burnout (BBO) and its relation to the microstructure of green tapes including the binder–plasticizer phase. Therefore, the article determines the shrinkage behavior of green tapes derived from alumina powders with different particle shape during binder burnout and prefiring in all spatial directions. The shrinkage after prefiring relative to the green and the debindered states is also discussed. The interrelation between shrinkage behavior and microstructure is investigated in dependence on different process parameters and specifically on the thermal behavior of the binder–plasticizer phase in the green tapes. It is shown that the subtraction of the BBO shrinkage from the total shrinkage results in completely different data for the sintering shrinkage anisotropy in z direction.

I. Introduction

Tape casting is a binder-assisted ceramic forming technique for the large-scale manufacture of sheets for various applications, such as, for example, capacitors, inductors, sensors, actuators, and high-integrated multilayer circuits.[1,2] These ceramic green tapes can be further processed via punching, metallization, and lamination to build-up complex multilayer products.[2] To enhance the green tape flexibility and strength, organic processing additives, such as binders and plasticizers are required.[3,4] Typically, the organic content ranges between 30 and 65 vol.% and is burned out prior to densification.[5]

During these processes, undesirable defects including delamination, cracks, anisotropic shrinkage, and camber can be observed,[3–5] which are attributed to anisotropic green tape microstructure caused by the forming process.[6–10] During tape casting, due to the shear flow gradient under the doctor blade nonequiaxed particles and binder molecules are oriented.[1,8] In addition, during the drying process, the solvent evaporation only occurs on the top surface. Due to the capillary forces, which transport the solvent to the surface, an increased amount of the dissolved binder can be found at the top surface of the tape.[2,5] Moreover, due to the adhesion forces between slurry and carrier tape, drying shrinkage can only be carried out in z direction, the direction perpendicular to the casting plane.[6–8] In summary, the anisotropic forming principle during tape casting results in particle orientation and in a textured and inhomogeneously distributed binder phase,[11] giving reason for an anisotropic pore structure after binder removal. These inhomogeneities in the green microstructure cause anisotropic shrinkage.[6–10]

$$\varepsilon_z \gg \varepsilon_y > \varepsilon_x \quad (1)$$

where ε represents the total linear sintering shrinkage relative to the green state and x, y and z denote the casting, transverse and thickness direction, respectively. In previous studies the effect of particle[6,7,11–13] and pore[14,15] orientation on the shrinkage anisotropy has been studied in detail. In this study, the shrinkage behavior of cast green tapes during binder burnout (BBO) and presintering were investigated quantitatively in all three spatial directions; special emphasis is given to the structural development during binder burnout.

II. Experimental Procedure

(1) Raw Materials

To determine the shrinkage behavior during binder burnout and prefiring, green tapes were cast using three different alumina powders of different particle shape. A spherical shaped powder (DAW 05, Denka Co., Ltd., Tokyo, Japan, d_{50}: 4.2 μm), a standard milled powder (WRA FG, Almatis GmbH, Frankfurt, Germany, d_{50}: 4.0 μm) and a platelet-shaped powder (P, Amis Co., Ltd., Sanmak-dong, Yangsan, South Korea, d_{50}: 8.7 μm) were used in this study.

(2) Slurry Preparation and Tape Casting

For tape casting, an azeotropic mixture of 68 wt.% ethanol and 32 wt.% toluene was used as solvent. After adding the dispersing agent (Fish oil, Kellogg Co., Buffalo, NY) and the Al_2O_3 powder, the dispersion was deagglomerated in a tumbling mixer (Turbula, Willy A. Bachofen AG, Muttenz, Switzerland) with Al_2O_3 milling balls (~30 wt.% of the slurry) with a diameter of ~3 mm for 24 h at a mixing speed of ~60 rpm. Then, the binder, polyvinylbutyral (PVB, B-98, Solutia Inc., St. Louis, MO) and the plasticizer, alkyl benzyl phtalate (Santicizer S261 A, Ferro Corp., Cleveland, OH) were added to the slurry. Subsequently, the suspension was homogenized for an additional 24 h, sieved through a screen of 200 μm and degassed (250 m bar, 30 min) to remove gas bubbles before casting. Table I shows the compositions of the tape casting slurries.

Tape casting was carried out on a tape casting machine equipped with a fixed double chamber casting head. A silicon-coated PET film (Mitsubishi Plastics, Inc., Tokyo, Japan) with a thickness of ~100 μm was used as a moving carrier. Drying was performed at room temperature without additional air flow. After drying, the ceramic green sheets were removed from the PET carrier film and cut to the desired sample sizes with a hot knife (Groz-Beckert KG, Albstadt, Germany) at 60°C. All green tapes used for the shrinkage analysis during binder burnout and prefiring, were cast at a casting speed of 300 mm/min. The front and rear doctor blades were adjusted to a gap height of 450 and 650 μm, respectively.

(3) Thermal Behavior of the Binder System

To characterize the thermal behavior of the binder–plasticizer system during thermal treatment, the mass loss and the heat of reaction of a WRA FG tape were determined by thermal

M. Mesuro—contributing editor

Manuscript No. 35237. Received July 1, 2014; approved September 3, 2014.
†Author to whom correspondence should be addressed. e-mail: andreas.roosen@fau.de

Journal of
Ceramic Science
and Technology

J. Ceram. Sci. Tech., 06 [02] 75-86 (2015)
DOI: 10.4416/JCST2015-00001
available online at: http://www.ceramic-science.com

Review

Additive Manufacturing of Bioactive Glasses and Silicate Bioceramics

R. Gmeiner[1], U. Deisinger[2], J. Schönherr[1], B. Lechner[1], R. Detsch[3], A. R. Boccaccini*[3], J. Stampfl[1]

[1]Inst. of Materials Science and Technology, Christian Doppler Laboratory: *Photopolymers in Digital and Restorative Dentistry*, Vienna University of Technology, A-1040 Vienna, Austria
[2]Institute of Glass and Ceramics, University of Erlangen-Nuremberg, D-91058 Erlangen, Germany; Current address: CeramTec GmbH, Medical Technology, D-91207 Lauf, Germany
[3]Institute of Biomaterials, University of Erlangen-Nuremberg, D-91058 Erlangen, Germany
received January 2, 2015; received in revised form March 4, 2015; accepted April 21, 2015

Abstract

This paper reviews the application of a broad range of additive manufacturing technologies (AMTs), including Stereolithographic Ceramic Manufacturing (SLCM/LCM), 3D-Printing, indirect and direct Selective Laser Sintering/Melting (SLS/SLM), Dispense Plotting and Inkjet Plotting on bioactive glasses (BGs) and silicate bioceramics to fabricate a variety of dense and porous structures for biomedical applications (e.g. bone replacement materials). Topical studies in the literature are complemented by recent data of the authors' own work, highlighting the state of the art of additive bioceramic production. The specific characteristics of the technologies used, their advantages and disadvantages and the scope for future research in this field are discussed. To date, many studies focus on 45S5 Bioglass® due to its broad commercial availability. However, other bioactive glass formulations and sol-gel derived BGs are being also considered in the context of AMTs. As the geometrical accuracy and mechanical properties of the fabricated parts strongly vary among the different AMTs, in-depth knowledge of the detailed capabilities of each production process targeted for BGs and other silicate bioceramic materials, as collated in this review, provides information on the basic requirements and challenges for establishing follow-up studies and for possible expansion of the application fields of such additive-manufactured structures.

Keywords: Additive manufacturing, bioactive glasses, silicate bioceramics, scaffolds

I. Introduction

Additive Manufacturing Technologies (AMTs) is the currently used standardized term for those processes (ASTM F2792) where 3D-structures are fabricated by adding material in the form of thin layers, to finally obtain the targeted geometry. In literature, the terms Rapid Prototyping, Layered Manufacturing, Solid Freeform Fabrication, 3D-Fabbing and 3D-printing are frequently used synonymously. In this work, the term AMT will be used, which describes the general manufacturing principle involved in the mentioned techniques.

There are two main categories of techniques to produce ceramic parts by AMT: direct and indirect fabrication techniques. Direct AMTs have the benefit of producing sintered ceramic parts without the need for any further thermal post-processing steps. These techniques melt the ceramic powder particles together by laser interaction and are referred to as selective laser sintering (SLS) [1,2] or electron beam melting (EBM). However, the obtained surfaces are usually rough and local thermal stress problems may arise because of temperature gradients [3] during production. Indirect methods to produce ceramic parts are three-step processes, consisting of three-dimensional printing, thermal debinding, and finally, sintering. Indirect methods involve four basic fabrication techniques, namely (i) laminated object manufacturing (LOM) [4,5], where the feedstock already includes the binder; (ii) extrusion-based techniques, such as robocasting, dispense-plotting and fused deposition modelling (FDM) [6]; (iii) methods relying on stereolithography, e.g. digital light processing (DLP) [7] or laser-based systems (SLA); and (iv) methods based on the fusing of a powder bed, such as 3D-printing and SLS methods, where the binder is present in the feedstock [8].

In general, AMTs are capable of shaping individual geometries on demand, without requiring expensive tooling. This makes AMTs ideal manufacturing processes for applications in medicine and biomedical engineering, where customized, patient-specific geometries are of high benefit. Fields of applications in current clinical use include the fabrication of drill guides for implantology and maxillo-facial surgery [9–12] as well as models [13] for digital dentistry. It is estimated that around 50 000 patients are treated every year using 3D-printed surgical planning instruments [14]. For these applications, the requirements regarding biocompatibility and bio-functional properties of the used materials are mostly achievable with currently avail-

* Corresponding author: aldo.boccaccini@ww.uni-erlangen.de

ADVANCED ENGINEERING MATERIALS

REVIEW

DOI: 10.1002/adem.201400110

Perspectives of Nano-Carbon Based Engineering Materials**

By *Peter Greil*

Nano-carbon materials attained considerable scientific interest due to their unique physico-chemical properties. Much less reports can be found on transferring the unique properties of super-strong individual nanoparticles like carbon nanotubes and graphene nanoplatelets into load bearing engineering materials. After reviewing structure and properties of nano-carbon properties the size effect governing the reduction of inherent mechanical properties upon transfer into macroscopic engineering materials is considered. While the potential of mechanical property enhancement of composites with random orientation of elongated carbon nanoparticles is limited by very low percolation thresholds, manufacturing of aligned microstructures, and tailoring of nanoparticle/matrix interface offers plenty of space for optimizing the mechanical properties of composites subjected to tensile loads. Since compression is the more common loading situation for ultra low-density nano-carbon materials the collapse stress is important for deriving design limits of nanoporous carbon materials. At the same level of density materials with nanotube or sheet carbon allotropes forming the struts may be expected to achieve a compression strength orders of magnitude higher than the porous graphitic materials. Finally, economic aspects of nano-carbon manufacturing are discussed.

1. Introduction

Distinguished by a low density, an outstanding chemical and thermal stability, as well as superior high temperature mechanical properties in non-oxidizing atmosphere, carbon is one of the most promising engineering materials. Carbon ($1s^2$, $2s^2$, and $2p^2$) is able to undergo flexible coordination chemistry forming sp (carbyne), sp^2 (graphite) and sp^3 (diamond) hybrid orbital bonding allowing formation of specific 3D architectures.[1] Carbon can be found in a wide variety of allotropes from crystalline (diamond and graphite) to amorphous (carbon black, activated carbon, glassy carbon, etc.) and nanoscale (fullerene, nanotube, graphene, and nanoporous), Table 1. Diamond and graphite are the crystalline carbon materials most relevant for engineering applications. Carbon fibers are prepared from organic precursors including stabilization of a precursor fiber in air (≈300 °C), carbonization (≈1100 °C), and subsequent graphitization (>2500 °C). Fibers undergoing only the first two steps are commonly called *carbon fibers*, while fibers undergoing all three steps are called *graphite fibers*.

In the past two decades, carbon forms with the characteristic sizes in the nanoscale region (e.g., one characteristic dimension is <100 nm) received increasingly attention due to their remarkable physico-chemical properties: fullerenes,[2] nanotubes,[3] nanofibers,[4] graphene,[5] nanodiamond,[6] and nanofoams.[7] Geometrical constraints on the nanoscale give rise for unique properties of nano-size carbon as, for example, quantum mechanical tunneling triggered field emission,[6] pore channel diameter controlled band gap in carbon nanotubes (CNTs), [8] helicity-dependent electrical conductance (metallic or semiconductor), [9] nanoporosity governed ultra low solid state thermal conductivity in carbon aerogels,[10] ultra high modulus and tensile strength of CNTs,[11] as well as tailored biological activity of functionalized fullerenes.[12] The wide diversity of nanosize carbon forms and architectures emphasizes the increasing role of

[*] *Prof. P. Greil*
Department of Materials Science (Glass and Ceramics), University of Erlangen-Nuernberg, Martensstr. 5, 91058 Erlangen, Germany

[**] *The financial support from the DFG funded Koselleck project GR 961/32 and the Cluster of Excellence "Engineering of Advanced Materials" is gratefully acknowledged.*

CrystEngComm

COMMUNICATION

View Article Online
View Journal | View Issue

Cite this: CrystEngComm, 2015, 17, 6831

Received 3rd March 2015,
Accepted 30th April 2015

DOI: 10.1039/c5ce00441a

www.rsc.org/crystengcomm

Pseudomorphic transformation of amorphous calcium carbonate films follows spherulitic growth mechanisms and can give rise to crystal lattice tilting†

Joe Harris,[a] I. Mey,[b] M. Hajir,[c] M. Mondeshki[c] and Stephan E. Wolf*[a]

Amorphous calcium carbonate films synthesized by the polymer-induced liquid-precursor (PILP) process convert into crystallographically complex calcite spherulites. Tuning the experimental parameters allows for the generation of crystal lattice tilting similar to that found in calcareous biominerals. This contribution evidences the role of spherulitic growth mechanisms in pseudomorphic transformations of calcium carbonate.

Calcareous biominerals, such as sea urchin spines and mollusk shells, are biogenically formed composite ceramics which show superb adaptation for given tasks. The 542 million years of evolution since the Cambrian explosion has rendered biominerals an immense source of inspiration for both material design and for the creation of ceramic materials at ambient temperature.[1] The key step during genesis of these biogenic ceramics is the controlled solid-amorphous to crystalline transformation from a transient precursor to a highly co-oriented mosaic crystal.[2–4] This phase transformation is pseudomorphic, *i.e.* it proceeds with conservation of the macro- and microscopic morphology of the mineral body which eventually leads to non-equilibrium shaped crystalline forms. For future mimesis of these intricate ceramics, the "percolation of crystallinity" through an initially fully amorphous mineral body has to be thoroughly understood. So far, it is generally accepted that biominerals initially form by aggregation of individual and amorphous nanoparticles.[4,5–8] In a subsequent state, crystallinity propagates[9] through the now fully aggregated[10,11] and anhydrous,[12] space-filling[13]/accreted[10,11] amorphous mineral body. This eventually generates a mosaic crystal with an insignificant angle spread, often referred to as a mesocrystal,‡[4,9,14,15] Ultrastructural analysis of different, mature calcareous biominerals revealed that they, in their fully crystalline state, still embody a nanogranular fine structure; a clear remnant of formation *via* aggregation and accretion processes of initially amorphous particles which eventually give rise to the conchoidal fracture behaviour of biominerals.[6,14–16] In extension to the recent work of Seto *et al.*,[14] Wolf *et al.* recently proposed that the apparent single crystallinity often observed in biominerals can be seen as an epitaxial nucleation process of the fundamental nanogranular building blocks, *i.e.* an already crystalline nanogranule bequeaths its crystal orientation to an adjacent and still amorphous granule by isoepitaxial nucleation.[15,16] Metaphorically speaking, crystallinity jumps to neighbouring granules and, by this, percolates through the entire mineral body eventually resulting in the formation of an apparently single-crystalline body. This speculative model, which still awaits further corroboration, is capable of explaining the emergence of single-crystallinity and also more peculiar observations recently made on biominerals, such as the preservation of intracrystalline amorphicity in biominerals as evidenced, for instance, by the Gilbert group by the use of XANES-PEEM mapping techniques.[9,12,16–18] In this special case, the revised model predicts that individual (patches of) nanogranules do not undergo phase transformation as they are either separated from the surrounding crystallinity by an impenetrable organic coating which ensheathes the granules or because their chemical composition does not meet the requirements, *e.g.* they contain too much water, foreign ions like magnesium, polymeric impurities, or improper stoichiometry.[16,19] Employing XANES-PEEM on an extensive set of nacroprismatic mollusks shells, Gilbert and co-workers recently found the first example of a structure–property relationship in biogenic calcitic prisms.[18] They observed a gradual tilting of the

[a] Department of Materials Science and Engineering, Chair of Glass and Ceramics (WW3), Friedrich-Alexander-University Erlangen-Nürnberg, Martensstrasse 5, 91058 Erlangen, Germany. E-mail: stephan.e.wolf@fau.de; Fax: +49 9131 85 28311; Tel: +49 9131 85 27585
[b] Institute of Organic and Biomolecular Chemistry, Georg-August-University of Göttingen, Tammannstrasse 2, 37077 Göttingen, Germany
[c] Institute of Inorganic and Analytical Chemistry, Johannes Gutenberg-University of Mainz, Duesbergweg 10-14, Germany

† Electronic supplementary information (ESI) available: Experimental details, polarized light micrographs of transient states of film formation; Raman, IR and PXRD analyses; line intensity profiles of type A and B spherulites; TGA/DSC profiles of spherulites; control crystallization experiments and AFM micrographs of the amorphous film. See DOI: 10.1039/c5ce00441a

nature COMMUNICATIONS

ARTICLE

Received 26 Jun 2015 | Accepted 3 Nov 2015 | Published 3 Dec 2015

DOI: 10.1038/ncomms10097 OPEN

Nanoscale assembly processes revealed in the nacroprismatic transition zone of *Pinna nobilis* mollusc shells

Robert Hovden[1,*], Stephan E. Wolf[2,3,*], Megan E. Holtz[1], Frédéric Marin[4], David A. Muller[1,5] & Lara A. Estroff[2,5]

Intricate biomineralization processes in molluscs engineer hierarchical structures with meso-, nano- and atomic architectures that give the final composite material exceptional mechanical strength and optical iridescence on the macroscale. This multiscale biological assembly inspires new synthetic routes to complex materials. Our investigation of the prism–nacre interface reveals nanoscale details governing the onset of nacre formation using high-resolution scanning transmission electron microscopy. A wedge-polishing technique provides unprecedented, large-area specimens required to span the entire interface. Within this region, we find a transition from nanofibrillar aggregation to irregular early-nacre layers, to well-ordered mature nacre suggesting the assembly process is driven by aggregation of nanoparticles (~50–80 nm) within an organic matrix that arrange in fibre-like polycrystalline configurations. The particle number increases successively and, when critical packing is reached, they merge into early-nacre platelets. These results give new insights into nacre formation and particle-accretion mechanisms that may be common to many calcareous biominerals.

[1] School of Applied and Engineering Physics, Cornell University, Ithaca, New York 14853, USA. [2] Department of Materials Science and Engineering, Cornell University, Ithaca, New York 14853, USA. [3] Department of Materials Science and Engineering, Institute of Glass and Ceramics, Friedrich-Alexander-University Erlangen-Nürnberg, 91058 Erlangen, Germany. [4] UMR CNRS 6282 Biogéosciences, Université de Bourgogne Franche-Comté, 6 Boulevard Gabriel, 21000 Dijon, France. [5] Kavli Institute at Cornell for Nanoscale Science, Ithaca, New York 14853, USA. * These authors contributed equally to this work. Correspondence and requests for materials should be addressed to L.A.E. (email: lae37@cornell.edu).

Journal of
Ceramic Science
and Technology

J. Ceram. Sci. Tech., 06 [02] 87-94 (2015)
DOI: 10.4416/JCST2015-00006
available online at: http://www.ceramic-science.com

Review

Fabrication of MAX-Phase-Based Ceramics by Three-Dimensional Printing

Y. Ma[1], X. Yin*[1], X. Fan[1], N. Travitzky[2], P. Greil[2]

[1]Science and Technology on Thermostructural Composite Materials Laboratory, Northwestern Polytechnical University, Xi¯an, Shaanxi, 710072, PR China
[2]Department of Materials Science (Glass and Ceramics), University of Erlangen-Nuremberg, Erlangen, Germany.

received February 3, 2015; received in revised form March 1, 2015; accepted April 1, 2015

Abstract

Three-dimensional printing (3DP) is a flexible and cost-effective method for direct digital manufacturing that provides capabilities for creating a wide range of part geometries in a broad variety of materials. Recently, a combined process of 3DP and reactive melt infiltration (RMI) has been applied to fabricate MAX-phase-based ceramics, exhibiting great potential in the fabrication of bulk compounds with complicated shape. This paper briefly summarizes the fabrication of Ti_3AlC_2- and Ti_3SiC_2-based ceramics with the combined process. 3DP facilitates the prior design of a porous preform with specific pore distribution and microstructure, which is beneficial to the control of the volume change of the following reaction in the RMI process, promoting the near-net-shape fabrication of MAX-phase-based ceramics with high flexibility in component geometry.

Keywords: Three-dimensional printing, RMI, Ti_3SiC_2, Ti_3AlC_2

I. Introduction

MAX phases are thermodynamically stable nanolaminates exhibiting unusual and unique properties. They have combined characteristics of metal and ceramics [1-3] and exhibit attractive properties such as good oxidation resistance, low density, high modulus, good thermal and electrical conductivity, excellent thermal shock resistance and high-temperature strength, and easy machinability [4-6]. They are considered promising structural/functional materials for high-temperature applications [7-9]. MAX phases have also been successfully used as reinforcement to improve the mechanical properties of intermetallic and ceramic-based composites [10].

Recently, several methods, such as chemical vapor deposition (CVD) [11,12], mechanical alloying (MA) [13,14], self-propagating high-temperature synthesis (SHS) [15-17], hot pressing (HP) [18] and spark plasma sintering (SPS) [13], have been applied to fabricate MAX-phase-based materials and the properties of these materials studied extensively.

Tzenov *et al.* [19] fabricated dense Ti_3AlC_2 bulk materials by means of reactive hot isostatic pressing (HIP) of a Ti, C, and Al_4C_3 powder mixture at 70 MPa, 1400 °C for 16 h. Yeh *et al.* [17] used a 3Ti/1.25C/0.25Al_4C_3 mixture as the starting powder to fabricate Ti_3AlC_2 ceramics by means of SHS, and the increase of the preform density prior to the SHS process led to the increase of Ti_3AlC_2 content from 50.5 to 73.2 wt%. Yanga *et al.* [13] combined MA and SPS methods for the fabrication of Ti_3AlC_2-based material. Dense Ti_3AlC_2 was fabricated by means of SPS at 1050 °C for 10 – 20 min with mechanically alloyed powders from a starting mixture of 3Ti/1.1Al/2C. Han *et al.* [20] fabricated polycrystalline bulk Ti_3AlC_2 with HP from a mixture of TiC_x (x = 0.6) and Al powder under 25 MPa pressure in the temperature range of 800 to 1600 °C, fully dense and pure Ti_3AlC_2 was synthesized by means of HP above 1400 °C; Vickers hardness up to 6 GPa and flexural strength higher than 900 MPa were measured for the as-fabricated bulk Ti_3AlC_2 samples.

CVD was the early method for the fabrication of dense Ti_3SiC_2 ceramics with high purity [11]. Deposition is usually conducted at 1300 – 1600 °C with $SiCl_4$, $TiCl_4$, CCl_4 and H_2 as source gases. However, CVD could only be used for the fabrication of thin films and coatings composed of MAX phases. Barsoum *et al.* [2] used the HIP method for the fabrication of bulk Ti_3SiC_2 materials. Powder blends of Ti, C and SiC with a molar ratio of 3:2:1 were cold-pressed under 180 MPa. In order to obtain dense materials, the compacted green bodies were then reacted in the HIP device at 1600 °C for 4 h under 40 MPa. Gao *et al.* fabricated dense Ti_3SiC_2 bulk material by means of SPS up to 1300 °C [21]. The composition of starting powder mixture was Ti:Si:TiC = 1:1:2 (molar ratio). The as-fabricated Ti_3SiC_2 material contained only 2 wt% TiC_x impurity. *In-situ* hot pressing was conducted by Zhou *et al.* [3] using mixed powders with a molar ratio of Ti:Si:C = 0.42:0.23:0.35. Ti_3SiC_2 bulk material with purity of 93 wt% was fabricated at 1550 °C in an atmosphere of flowing Ar. Further study [22] shows that using

* Corresponding author: yinxw@nwpu.edu.cn

Int. J. Appl. Ceram. Technol., 12 [1] 71–80 (2015)
DOI:10.1111/ijac.12321

Near-Net-Shape Fabrication of Ti_3SiC_2-based Ceramics by Three-Dimensional Printing

Yuzhao Ma, Xiaowei Yin,* Xiaomeng Fan, and Lei Wang

Science and Technology on Thermostructural Composite Materials Laboratory, Northwestern Polytechnical University, Xi'an, Shaanxi 710072, People's Republic of China

Peter Greil and Nahum Travitzky*

Department of Materials Science (Glass and Ceramics), University of Erlangen-Nuremberg, Erlangen 91058, Germany

This paper focuses on the preparation of near-net-shaped dense Ti_3SiC_2-based materials via an indirect three-dimensional printing (3D printing) and postreactive melt infiltration (RMI) processes. TiC preforms with bimodal pore size distribution were fabricated through 3D printing, followed by the infiltration of Si melt and Al–Si alloy ($Al_{40}Si_{60}$ and $Al_{70}Si_{30}$). Dense composites with density of ~4.1 g/cm^3 were obtained after the infiltration. No volume shrinkage was obtained after the reactive infiltration with Al–Si alloy. The participation of Al during the infiltration process promoted the formation of Ti_3SiC_2. The as-fabricated Ti_3SiC_2-based materials showed enhanced mechanical and electromagnetic interference shielding properties.

Introduction

Ti_3SiC_2 is the representative and most studied phase among the $M_{n+1}AX_n$ ternary compounds.[1,2] It combines characteristics of metal and ceramics due to its metallic nature of bonding and layered nature of compounds and attains attractive properties such as good oxidation resistance, low density, high modulus, good thermal and electrical conductivity, excellent thermal shock resistance and high temperature strength, and easy machinability.[3–5] It has also been considered as a promising structural/functional material which would be used in the high-temperature conditions.[6–8] The microwave and electromagnetic interference (EMI) shielding properties of Ti_3SiC_2 are attracting more and more attentions. Shi *et al.*[9] demonstrated that the EMI SE (shielding effectiveness) of the Ti_3SiC_2/polyaniline composites in X-band can be greatly improved by increasing Ti_3SiC_2 filler content. Liu[10] and Li[11] *et al.* also studied the dielectric and microwave absorption properties of Ti_3SiC_2 powders. The authors showed that Ti_3SiC_2 is good microwave absorbent in X-band. However, up to now, MAX-phase-based materials were still prepared mainly by the traditional process of hot-pressing at elevated temperatures with limited shaping capability to rather simple component geometries.[12,13]

Additive manufacturing is a novel processing technology of ceramic-based materials, which have the capacity to combine geometry design with material design.[14] Three-dimensional printing (3D printing) is a promising additive manufacturing technology that allows the rapid flexible production of prototype parts from a CAD model.[15] 3D printing directly employs powders and binders to create complex shape ceramic parts with no tooling or geometric limitation. Although 3D printing has the unique ability to locally tailor the material composition, microstructure, and surface texture, it remains a challenging issue for creating dense ceramics using 3D printing technology. Sun *et al.*[16] used cold-isotactic pressing for the densification of the 3D printed Ti_3SiC_2 samples. Fu *et al.*[17] fabricated SiSiC lattice structures with a gradient by 3D printing, preceramic polymer infiltration, and pressureless liquid Si infiltration. After Si melt infiltration, the SiSiC composites show a dense microstructure up to 70 vol% of Si. Schlier *et al.*[18] used 3D printing combined for the fabrication of SiSiC macrocellular lattice truss structures for free combustion process. The lattice design with a high porosity of 80% was shaped by indirect three-dimensional printing.

3D printing is demonstrated to be an enable process to fabricate porous preforms with carefully designed porosity and pore size distribution, which is beneficial to the formation of a dense MAX-phase-based ceramics by a postmetal reactive infiltration (RMI).[19–22] In our previous works,[19] Ti_3SiC_2-based ceramics were fabricated by liquid silicon infiltration into 3D printing TiC preforms with a bimodal pores structure which favors the infiltration with liquid melt. The as-obtained ceramics gained

*xiaow@nwpu.edu.cn, yinxiaowei@yahoo.com, nahum.travitzky@ww.uni-erlangen.de

JOURNAL OF APPLIED PHYSICS 118, 164104 (2015)

In-situ structural investigations of ferroelasticity in soft and hard rhombohedral and tetragonal PZT

Maxim I. Morozov,[1,a)] Mari-Ann Einarsrud,[1] Julian R. Tolchard,[1] Philipp T. Geiger,[2] Kyle G. Webber,[2] Dragan Damjanovic,[3] and Tor Grande[1]
[1]*Department of Materials Science and Engineering, Norwegian University of Science and Technology, NO-7491 Trondheim, Norway*
[2]*Department of Materials Science, Friedrich-Alexander-Universität Erlangen-Nürnberg, 91058 Erlangen, Germany*
[3]*Ceramics Laboratory, Swiss Federal Institute of Technology in Lausanne-EPFL, 1015 Lausanne, Switzerland*

(Received 14 September 2015; accepted 13 October 2015; published online 28 October 2015)

Despite the technological importance of hard and soft PZT, $Pb(Zr,Ti)O_3$, ceramics, the mechanisms of ferroelectric hardening and softening remain widely discussed in the literature. The hardening and softening phenomena have traditionally been investigated in relation with dielectric manifestations such as aging of the dielectric susceptibility and constriction of the polarization-electric field hysteresis loop. Here, we present a systematic investigation of the ferroelectric and ferroelastic properties of soft and hard PZT in both the tetragonal and rhombohedral phases. A particular focus has been devoted to ferroelastic domain switching by characterizing the macroscopic mechanical constitutive behavior and *in-situ* synchrotron X-ray diffraction during compression. It is demonstrated that variation of the ordering state of point defects in PZT ceramics affects the switching behavior of both ferroelectric and ferroelastic domains under mechanical or electrical fields. Softening of the mechanical and electrical properties of originally hard PZT ceramics was conferred by quenching the materials from above the Curie temperature. The present findings are discussed with respect to the current understanding of hardening-softening transitions in ferroelectric materials. © *2015 AIP Publishing LLC*. [http://dx.doi.org/10.1063/1.4934615]

I. INTRODUCTION

Introduction of donor or acceptor dopants in lead zirconate titanate (PZT) is one of the most successful methods to tailor the piezoelectric and ferroelectric performance of these electroceramics.[1] Aliovalent dopants can control both the intrinsic and extrinsic properties such as bulk electric conductivity and mobility of domain walls. Acceptor doping is known to induce ferroelectric "hardening," i.e., weakening of dielectric and electromechanical properties, accompanied with lowering their nonlinearity and hysteresis. In contrast, donor dopants typically result in "softening" effects with the opposite tendencies. Many theoretical and experimental studies have been dedicated to these phenomena, and several models have been proposed to describe the dielectric nonlinearity and hysteresis using phenomenological, micromechanical, and statistical simulations.

The phenomenological models of "hardening" usually consider interaction between the spontaneous polarization (P_S) and charged point defects, whose collective ordering or localization results in pinning of domain walls, hence reducing their mobility. Several models with different localizations of charged point defects (in some models—space charge) have been proposed and discussed extensively.[2–16] Ordering of charged point defects with respect to polarization is a result of their interaction with P_S at elevated temperatures below the Curie temperature, T_C. Migration and rearrangement of mobile point defects may occur quickly[17,18] at the last stage of thermal processing, when sintered ceramics first reach the polar state on cooling below T_C. At room temperature, the ordered arrangement of the point defects is considered to be "frozen"; thus, their collective interaction with P_S tends to hold the domain configuration stable, manifesting itself as a "restoring force" for the motion of weak domain walls. In the case of "hard" acceptor-doped ceramics, positively charged oxygen vacancies $V_O^{\bullet\bullet}$ appear to balance partially or completely[18–20] the negatively charged acceptors. Due to certain mobility below the Curie temperature (e.g., in PZT, $T_C > 300$ °C), $V_O^{\bullet\bullet}$–acceptor pairs may adopt preferential sites in the unit cells with respect to the spontaneous polarization of the ferroelectric domains. Thus, the level of charged point defect ordering can be a measure of ferroelectric hardening.

Unlike "hardening," the "softening" mechanism is still poorly understood. It is believed that the undoped ceramics are "hard" to a certain extent, i.e., due to the presence of $V_O^{\bullet\bullet}$ mainly owing to the loss of PbO. The $V''_{Pb} - V_O^{\bullet\bullet}$ pair then has a similar role in hardening as the acceptor dopant-oxygen vacancy cluster. The introduction of donor dopants (i.e., Nb^{5+}) reduces this natural ferroelectric "hardness" by reducing the number of oxygen vacancies and thus manifests itself as softening. Whether any additional softening effects, beyond the decrease in concentration of oxygen vacancies, are present is currently not understood. The softening donor-type dopants in PZT are typically cation substitutes (e.g., $Nb^{\bullet}_{(Zr,Ti)}$) balanced by cation vacancies (e.g., V''_{Pb}). These two point defects are considered to be immobile compared to oxygen vacancies at temperatures below T_C; thus, they are not able to become ordered with the onset of the spontaneous

a)Author to whom correspondence should be addressed. Electronic mail: maximm@alumni.ntnu.no

Acta Biomaterialia 23 (2015) 317–328

Contents lists available at ScienceDirect

Acta Biomaterialia

journal homepage: www.elsevier.com/locate/actabiomat

Freeze gelated porous membranes for periodontal tissue regeneration

Saad B. Qasim [a], Robin M. Delaine-Smith [b], Tobias Fey [c], Andrew Rawlinson [d], Ihtesham Ur Rehman [a,*]

[a] Materials Science and Engineering Department, Kroto Research Institute, University of Sheffield, Sheffield S3 7HQ, United Kingdom
[b] Institute of Bioengineering, School of Engineering and Materials Science, Queen Mary University of London, Mile End Road, E1 4NS London, United Kingdom
[c] Department of Materials Science (Glass and Ceramics), University of Erlangen-Nuremberg, Martensstr. 5, 91058 Erlangen, Germany
[d] Academic Unit of Restorative Dentistry, School of Clinical Dentistry, University of Sheffield, Sheffield S10 2SZ, United Kingdom

ARTICLE INFO

Article history:
Received 11 January 2015
Received in revised form 2 April 2015
Accepted 4 May 2015
Available online 9 May 2015

Keywords:
Ascorbic acid
Guided tissue regeneration
Resorbable
Bioactivity
Osteoblasts

ABSTRACT

Guided tissue regeneration (GTR) membranes have been used for the management of destructive forms of periodontal disease as a means of aiding regeneration of lost supporting tissues, including the alveolar bone, cementum, gingiva and periodontal ligaments (PDL). Currently available GTR membranes are either non-biodegradable, requiring a second surgery for removal, or biodegradable. The mechanical and biofunctional limitations of currently available membranes result in a limited and unpredictable treatment outcome in terms of periodontal tissue regeneration. In this study, porous membranes of chitosan (CH) were fabricated with or without hydroxyapatite (HA) using the simple technique of freeze gelation (FG) via two different solvents systems, acetic acid (ACa) or ascorbic acid (ASa). The aim was to prepare porous membranes to be used for GTR to improve periodontal regeneration. FG membranes were characterized for ultra-structural morphology, physiochemical properties, water uptake, degradation, mechanical properties, and biocompatibility with mature and progenitor osteogenic cells. Fourier transform infrared (FTIR) spectroscopy confirmed the presence of hydroxyapatite and its interaction with chitosan. μCT analysis showed membranes had 85–77% porosity. Mechanical properties and degradation rate were affected by solvent type and the presence of hydroxyapatite. Culture of human osteosarcoma cells (MG63) and human embryonic stem cell-derived mesenchymal progenitors (hES-MPs) showed that all membranes supported cell proliferation and long term matrix deposition was supported by HA incorporated membranes. These CH and HA composite membranes show their potential use for GTR applications in periodontal lesions and in addition FG membranes could be further tuned to achieve characteristics desirable of a GTR membrane for periodontal regeneration.

1. Introduction

Destructive forms of periodontal disease such as chronic periodontitis affect the supporting tissues of teeth causing loss of gingival tissue, connective tissue, alveolar bone and periodontal ligaments. Initial treatment of these diseases includes the elimination of the primary causative factor (the dental plaque biofilm) by effective patient performed oral hygiene procedures and non-surgical treatment provided by a dentist or hygienist. While treatment usually halts disease progression, healing is characterized by repair of affected tissues with a long junctional epithelium, bone remodeling, and limited regeneration of the cementum and the lost periodontal ligaments that normally attach the tooth to the alveolar bone.

For these reasons, there has been much interest in developing methods for enhancing the regeneration of lost tissues in order to restore dental function and esthetics. This has been met with limited success using biologically active agents and guided tissue regenerative (GTR) or guided bone regeneration (GBR) membranes [1,2]. The ideal requirements for a GTR membrane include; a cell isolating occlusive biomaterial which meets minimum mechanical, physical, structural and biocompatibility requirements; ability to support organized and vascularized ingrowth and wound stabilization; protecting the underlying blood clot and thereby limiting the epithelial and unwanted connective tissue growth into the defect; promoting functional tissue regeneration from the relevant cells in the defect (avoiding healing by repair); and degrading in adequate time to provide space for newly formed periodontal tissue. The membrane surface facing the soft tissue should support cell attachment, growth and differentiation while the surface facing the defect acts as a biological seal [3].

A number of resorbable GTR/GBR membranes have now replaced the conventional non-resorbable membrane (expanded

* Corresponding author at: The Kroto Research Institute, North Campus, University of Sheffield, Broad Lane, Sheffield S3 7HQ, United Kingdom. Tel.: +44 (0) 114 222 5946; fax: +44 (0) 114 222 5943.
E-mail address: i.u.rehman@sheffield.ac.uk (I.U. Rehman).

http://dx.doi.org/10.1016/j.actbio.2015.05.001
1742-7061/

Article

JOURNAL OF COMPOSITE MATERIALS

Journal of Composite Materials
2015, Vol. 49(16) 1971–1976

DOI: 10.1177/0021998314541307
jcm.sagepub.com
SAGE

Conductive TiC/Ti–Cu/C composites fabricated by Ti–Cu alloy reactive infiltration into 3D-printed carbon performs

Carlos R Rambo[1], Nahum Travitzky[2] and Peter Greil[2]

Abstract

The microstructure and electrical properties of dense TiC/Ti–Cu/C composites fabricated by pressureless reactive infiltration of Ti–Cu alloy into porous starch-derived carbon preforms prepared by 3D printing was evaluated. Porosities in the range of 65–78 vol% were varied by post-isostatic pressing the as-printed preforms at pressures of 50–400 MPa. The reactive melt infiltration was carried out at 1100 °C in a flowing Ar atmosphere and resulted in formation of a composite comprised predominantly of substoichiometric TiC, binary intermetallic Ti–Cu phases and residual carbon. Scanning electron microscopy analyses revealed a microstructure consisting of dispersed fine-grained TiC in a Ti–Cu matrix surrounded by a continuous carbon phase. Electrical resistivity measurements using the four-probe method were carried out and correlated to the composite microstructure. The electrical resistivity was evaluated in terms of carbon and TiC volume fractions.

Keywords

TiC/Ti–Cu/C composites, Ti–Cu alloy, 3D printing, reactive infiltration

Introduction

Ceramic particle-reinforced metal matrix composites (MMCs) are potential candidates for defence, automobile, aerospace, among several industrial applications. During the last decades, several processing routes were developed in order to decrease production costs and achieve adequate properties of advanced MMCs.[1–3] High temperature, hard MMCs with a wide range of compositions and controlled microstructure can be produced by compaction and forming of metal–ceramic powders.[4–6] Kaftelen et al.[4] produced Al–Cu matrix composites reinforced with TiC particulates by two distinct routes: mechanical alloying and flux-assisted casting of TiC and Al–4 wt.% Cu alloy mixtures. Powder processing approaches offer a variety of advantages; however, they are limited by slow and costly forming, consolidation and machining production steps. Alternatively, melt casting processes offer the possibility to produce dense composites with complex and near-net shapes in short time processing. On the other hand, melt casting of MMCs with fine and continuous ceramic phase is also an expensive and relatively complex route that demands high temperature processing (≥1200 °C) or high infiltration pressures.[7]

The casting temperature and processing time can be substantially reduced by reactive infiltration processes, where the ceramic phase is then in situ formed through a simultaneous infiltration and reaction of a molten metal with the solid porous preform. Several processing routes based on in situ production of MMCs have been reported that resulted in the formation of a very fine, interpenetrating and thermodynamically stable reinforcing ceramic phase within an intermetallic matrix.[8–12] Al alloys (Al–Si, Al–Ti) and metallic Ti and Si are the most used for producing MMCs with carbide phases as

[1]Department of Electrical Engineering, Federal University of Santa Catarina, Florianópolis, Brazil
[2]Department of Materials Science, Glass and Ceramics, University of Erlangen-Nuernberg, Erlangen, Germany

Corresponding author:
Carlos R Rambo, Department of Electrical Engineering, Federal University of Santa Catarina, Florianópolis, Brazil.
Email: rambo@eel.ufsc.br

Scripta Materialia 108 (2015) 84–87

Contents lists available at ScienceDirect

Scripta Materialia

journal homepage: www.elsevier.com/locate/scriptamat

Local densification of a single micron sized silica sphere by uniaxial compression

Stefan Romeis [a], Jonas Paul [a], Patrick Herre [a], Dominique de Ligny [b], Jochen Schmidt [a,*], Wolfgang Peukert [a]

[a] Institute of Particle Technology, Friedrich-Alexander-Universität Erlangen-Nürnberg, Cauerstraße 4, 91058 Erlangen, Germany
[b] Institute of Glass and Ceramics, Friedrich-Alexander-Universität Erlangen-Nürnberg, Martensstraße 5, 91058 Erlangen, Germany

ARTICLE INFO

Article history:
Received 30 April 2015
Revised 19 May 2015
Accepted 14 June 2015
Available online 15 June 2015

Keywords:
Silica glass
Scanning electron microscopy (SEM)
Raman spectroscopy
Deformation structure
Plastic deformation

ABSTRACT

In situ uniaxial compression experiments are performed inside a SEM for compact vitreous SiO_2 microparticles. The local structure of a plastically deformed particle is assessed spatially resolved *ex situ* by micro Raman spectroscopy. By application of a density calibration curve a maximum silica network densification of 11% is found only in zones slightly below the circular contact areas. The particle's inner regions remain unaffected. Conclusions from geometric considerations indicate that the observed plasticity during compression is completely accommodated by local densification.

Commonly, silica glasses are perceived as brittle materials. However, at length scales beneath some microns and under very high pressures, glasses can be permanently deformed [1–3]. Plastic deformation of glasses is associated with volume conservative shear flows and permanent densification of the network [4]. Densification is accommodated, at the expense of the free molar volume, by rearrangements of the glass network on the intermediate structural level (polyamorphic transition) [5]. The free molar volume which varies with the atomic packing density and the Poisson ratio has been identified as a key parameter for the possible maximum densification [6]: highly polymerized structures (open networks with low atomic packing densities and Poisson ratios) can be greatly densified; the overall achievable densification is significantly reduced for depolymerized glasses (higher atomic packing densities and Poisson ratios) [6]. The densification increases gradually with applied pressure between a lower elastic pressure limit and an upper saturation pressure. For the hydrostatic compression of silica the lower threshold is ~10 GPa; saturation occurs at ~25 GPa and at a densification of 21% [7]. Structural compaction can also be induced by irradiation from various sources (including electrons); the maximum densification is limited to 3% [8–12]. The structure of glasses at intermediate length scales can be studied by Raman spectroscopy. Accurate links between the permanent densification from pressure compaction and the corresponding Raman spectra have been established [13,14]. During hydrostatic compression of glasses only structural compaction is observed. For more complex loading situations (e.g. indentation or uniaxial compression) plastic deformation might be accommodated by a combination of volume conservative shear flows and pressure compaction of the silica network. The relative contributions of the aforementioned mechanisms depend on the actual stress in the material. Clearly, the confined volumes encountered e.g. in nanoindentation behave differently than particles with free surface – an example for the deconfinement of particles has recently been given e.g. for silicon [15]. Different (particle) geometries might thus be an ideal testing case for the currently available constituent models describing glass deformation [16,17]. However, mainly the local densification induced by indentation is being studied [13,17,18]. Although well-established e.g. for metallic glasses, pillar testing has hardly been employed for silica glasses. In the studies by Lacroix et al. [19,20] the permanent deformation of compressed silica pillars was completely attributed to shear flows; a direct characterization of the resulting glass structure after compression is not given. Several recent studies evidence a high plasticity of micron sized spherical silica particles [3,21,22]. However, the local structure of the compressed particles has not been characterized and the underlying deformation modes are still unknown.

Within this contribution, we study the local densification of a plastically deformed single vitreous silica microsphere. Uniaxial compression of the single silica particle is performed by a SEM

* Corresponding author.
E-mail address: jochen.schmidt@fau.de (J. Schmidt).

http://dx.doi.org/10.1016/j.scriptamat.2015.06.023
1359-6462/

Available online at www.sciencedirect.com

ScienceDirect

Ceramics International 41 (2015) 12595–12603

CERAMICS INTERNATIONAL

www.elsevier.com/locate/ceramint

Processing and characterization of paper-derived Ti_3SiC_2 based ceramic

Jan Schultheiß[a], Benjamin Dermeik[a,*], Ina Filbert-Demut[a], Nils Hock[a], Xiaowei Yin[b], Peter Greil[a], Nahum Travitzky[a,*]

[a]University of Erlangen—Nuremberg, Department of Materials Science (Glass and Ceramics), Martensstr. 5, Erlangen D-91058, Germany
[b]Northwestern Polytechnical University, Science and Technology on Thermostructure Composite Materials Laboratory, Xi'an 710072, Shaanxi, People's Republic of China

Received 22 April 2015; received in revised form 10 June 2015; accepted 18 June 2015
Available online 26 June 2015

Abstract

Porous layers of paper-derived titanium silicon carbide (Ti_3SiC_2), with a thickness ranging from 300 to 700 μm, were obtained by the heat treatment of preceramic papers containing Ti_3SiC_2 as filler particles. The tearing strength of the preceramic papers was provided by cellulose fibers obtained from wood by the kraft pulping process, also described as pulp fibers, and ionic starches. Short pulp fibers with an average length of 657 μm were derived from short fibered hardwood (eucalyptus), while long pulp fibers with an average length of 1665 μm were derived from long fibered softwood (spruce, pine and larch). The fiber length of pulp fibers in the preceramic papers also influenced the microstructure and the properties of the paper-derived Ti_3SiC_2. Preceramic papers fabricated with short pulp fibers exclusively led to an average porosity of 18.6 vol% for the paper-derived Ti_3SiC_2, whereas the paper-derived Ti_3SiC_2 had an average porosity of 45.3 vol% when preceramic papers with long pulp fibers only were used. The density of the paper-derived Ti_3SiC_2 also affected the flexural strength, as could be shown by densifying preceramic papers using a calender. Thereby, the flexural strength of paper-derived Ti_3SiC_2 could be increased by more than five times, from 13 MPa to 83 MPa. The purity of the paper-derived Ti_3SiC_2 was found to be dependent on the purity of the raw materials and the process cycle, with TiC_x and Al_2O_3 impurities present in the ceramics.

Keywords: A. Sintering; A. Shaping; C. Mechanical properties; D. Carbides; MAX-phase

1. Introduction

Ceramics are the materials of choice for lightweight structures and for high-temperature applications. Shaping of ceramic materials is one of the key issues in the manufacturing of lightweight structures. Important progress referring to this topic has been made with the fabrication of paper-derived ceramics starting with preceramic paper as a preform [1]. In this system, the preceramic paper is paper filled with at least 80 wt% of inorganic fillers. Paper-derived ceramics are obtained by heat treatment of preceramic papers. This has several advantages in comparison to conventional routes of ceramic processing. With well-established paper forming techniques the preforms can be shaped into multilayer laminates or more complex shapes, such as corrugated board structures or multi-wound roll structures. Additionally, the amount of porosity and the average pore size can be controlled by the composition of raw materials. Three-dimensional objects can be generated by employing laminated object manufacturing (LOM), a process in which preceramic paper sheets are sequentially stacked, laminated and shaped [2].

The aim of this work was the novel fabrication of Ti_3SiC_2 as a paper-derived MAX phase by the heat treatment of preceramic papers with Ti_3SiC_2 particles as ceramic filler. Ti_3SiC_2 is a representative and well-studied compound among the nano-laminated $M_{n+1}AX_n$ ternary compounds. It combines typical properties of metals and ceramics due to its low density, high modulus, good thermal and electrical conductivity, good oxidation

*Corresponding authors at: Department of Materials Science (Glass and Ceramics), University of Erlangen—Nuremberg, Martensstr. 5, 91058 Erlangen, Germany. Tel.: +49 9131 85 27561/+49 9131 85 28775; fax: +49 9131 8528311.
E-mail addresses: benjamin.dermeik@fau.de (B. Dermeik), nahum.travitzky@fau.de (N. Travitzky).

http://dx.doi.org/10.1016/j.ceramint.2015.06.085
0272-8842/

International Journal of Nanomedicine

Dovepress

ORIGINAL RESEARCH

Hypericin-bearing magnetic iron oxide nanoparticles for selective drug delivery in photodynamic therapy

Harald Unterweger[1]
Daniel Subatzus[1]
Rainer Tietze[1]
Christina Janko[1]
Marina Poettler[1]
Alfons Stiegelschmitt[2]
Matthias Schuster[3]
Caroline Maake[4]
Aldo R Boccaccini[5]
Christoph Alexiou[1]

[1]ENT Department, Section of Experimental Oncology and Nanomedicine (SEON), Else Kröner-Fresenius-Stiftung Professorship, University Hospital Erlangen; [2]Institute of Glass and Ceramics, Department of Materials Science and Engineering, University Erlangen-Nuremberg, [3]Materials for Electronics and Energy Technology, Department of Materials Science and Engineering, University Erlangen-Nürnberg, Erlangen, Germany; [4]Institute of Anatomy, University of Zurich, Winterthurerstr, Zurich, Switzerland; [5]Institute of Biomaterials, Department of Materials Science and Engineering, University Erlangen-Nuremberg, Erlangen, Germany

Correspondence: Christoph Alexiou
ENT-Department, Section of Experimental Oncology and Nanomedicine, HNO Klinik, Else Kröner-Fresenius-Stiftung Professorship, University Hospital Erlangen, Waldstraße 1 1, 91054 Erlangen, Germany
Tel +49 9131 8534769
Fax +49 9131 8534808
Email c.alexiou@web.de

Abstract: Combining the concept of magnetic drug targeting and photodynamic therapy is a promising approach for the treatment of cancer. A high selectivity as well as significant fewer side effects can be achieved by this method, since the therapeutic treatment only takes place in the area where accumulation of the particles by an external electromagnet and radiation by a laser system overlap. In this article, a novel hypericin-bearing drug delivery system has been developed by synthesis of superparamagnetic iron oxide nanoparticles (SPIONs) with a hypericin-linked functionalized dextran coating. For that, sterically stabilized dextran-coated SPIONs were produced by coprecipitation and crosslinking with epichlorohydrin to enhance stability. Carboxymethylation of the dextran shell provided a functionalized platform for linking hypericin via glutaraldehyde. Particle sizes obtained by dynamic light scattering were in a range of 55–85 nm, whereas investigation of single magnetite or maghemite particle diameter was performed by transmission electron microscopy and X-ray diffraction and resulted in approximately 4.5–5.0 nm. Surface chemistry of those particles was evaluated by Fourier transform infrared spectroscopy and ζ potential measurements, indicating successful functionalization and dispersal stabilization due to a mixture of steric and electrostatic repulsion. Flow cytometry revealed no toxicity of pure nanoparticles as well as hypericin without exposure to light on Jurkat T-cells, whereas the combination of hypericin, alone or loaded on particles, with light-induced cell death in a concentration and exposure time-dependent manner due to the generation of reactive oxygen species. In conclusion, the combination of SPIONs' targeting abilities with hypericin's phototoxic properties represents a promising approach for merging magnetic drug targeting with photodynamic therapy for the treatment of cancer.

Keywords: magnetic drug targeting, photodynamic therapy, SPION, hypericin

Introduction

One of the most promising approaches for cancer treatment in the last few years is magnetic drug targeting (MDT).[1–3] In this concept, drug accumulation in the tumor can be achieved with a drug-loaded magnetic carrier system, which is physically directed to the region of interest by an external magnetic field.[4,5] In comparison to conventional drug administration, this leads to an effective increase in the drug concentration in the affected tissue as well as a reduced drug concentration in the rest of the body.[6,7] Thus, a decrease in systemic side effects, such as nausea, hair loss, or neurotoxicity, can be achieved.[8–10]

An interesting feature of MDT is that it can be combined with other cancer treatment strategies such as photodynamic therapy (PDT), to create an even more selective treatment. Magnetic particles that are commonly used for MDT are superparamagnetic iron oxide nanoparticles (SPIONs), including magnetite (Fe_3O_4),

Engineering Fracture Mechanics 144 (2015) 68–77

Contents lists available at ScienceDirect

Engineering Fracture Mechanics

journal homepage: www.elsevier.com/locate/engfracmech

Temperature-dependent *R*-curve behavior of the lead-free ferroelectric $0.615Ba(Zr_{0.2}Ti_{0.8})O_3$–$0.385(Ba_{0.7}Ca_{0.3})TiO_3$ ceramic

Malte Vögler [a,*], Matias Acosta [a], David R.J. Brandt [a], Leopoldo Molina-Luna [a], Kyle G. Webber [a,b]

[a] Institute of Materials Science, Technische Universität Darmstadt, 64287 Darmstadt, Germany
[b] Department of Materials Science, Friedrich-Alexander-Universität Erlangen-Nürnberg, 91058 Erlangen, Germany

ARTICLE INFO

Article history:
Received 11 November 2014
Received in revised form 19 June 2015
Accepted 23 June 2015
Available online 26 June 2015

Keywords:
Fracture mechanics
Crack growth
R-curve
BZT–BCT
Ferroelastic

ABSTRACT

The temperature-dependent crack growth resistance behavior of the lead-free $(1-x)Ba(Zr_{0.2}Ti_{0.8})O_3$–$x(Ba_{0.7}Ca_{0.3})TiO_3$ ($x = 0.385$) ceramic was characterized using compact-tension specimens from 25 °C to 60 °C. The observed plateau fracture toughness at 25 °C was found to be approximately 37% lower than commercial $Pb(Zr,Ti)O_3$. At elevated temperature, the maximum fracture toughness displayed a decrease, which was found to be related to the temperature-dependent elastic and ferroelastic properties. Mechanical measurements are presented that demonstrate decreasing effective switching strain, coercive stress and Young's modulus with increasing temperature.

1. Introduction

Lead zirconate titanate ($Pb(Zr,Ti)O_3$, PZT) is the most commercially important piezoelectric ceramic due to the excellent dielectric, ferroelectric and piezoelectric properties. A significant downside of PZT, however, is the toxicity of lead, which is restricted by various international regulations, such as "Restriction of the Use of Certain Hazardous Substances in Electrical and Electronic Equipment (RoHS)" by the European Union [1]. The search for lead-free alternatives has revealed some promising candidates, such as $(Bi_{0.5}Na_{0.5})TiO_3$–$BaTiO_3$ (BNT–BT) [2,3], $(Bi_{0.5}Na_{0.5})TiO_3$–$(Bi_{0.5}K_{0.5})TiO_3$ (BNT–BKT) [4–7] and $(K_{0.5}Na_{0.5})NbO_3$ (KNN) [8–11]. The $(1-x)Ba(Zr_{0.2}Ti_{0.8})O_3$–$x(Ba_{0.7}Ca_{0.3})TiO_3$ (BZT–BCT) system was discovered by McQuarrie and Behnke [12] in 1954. Nevertheless, its potential for electromechanical applications was only recently realized by Liu and Ren [13]. Due to the high piezoelectric properties it has been proposed as a potential replacement for PZT in applications with low operating temperatures, like precision probe stages, thread guides, or vacuum circuit breakers [14–18]. A special feature of the BZT–BCT system is its polymorphic phase boundary (PPB). First publications reported a room temperature rhombohedral–tetragonal phase transition at a composition of about BZT–50BCT [13,19]. More recent studies suggest an intermediate phase [20–22], which was suggested by Keeble et al. [23] to be orthorhombic. Analogous to other piezoelectric ceramics, the transition region is of particularly high interest since the dielectric and piezoelectric properties are enhanced in its vicinity [24].

* Corresponding author at: Technische Universität Darmstadt, FB Nichtmetallisch-Anorganische Werkstoffe, Alarich-Weiss-Strasse 2, D-64287 Darmstadt, Germany. Tel.: +49 6151 16 21687.
E-mail address: voegler@ceramics.tu-darmstadt.de (M. Vögler).

http://dx.doi.org/10.1016/j.engfracmech.2015.06.069
0013-7944/

Available online at www.sciencedirect.com

ScienceDirect

Journal of the European Ceramic Society 35 (2015) 2321–2332

www.elsevier.com/locate/jeurceramsoc

Manufacture of sub-μm thin, particulate-based ITO layers by roller coating

Moritz Wegener, Denise Eckert, Andreas Roosen *

University of Erlangen-Nuremberg, Department of Materials Science, Glass and Ceramics, 91058 Erlangen, Germany

Received 20 August 2014; received in revised form 11 February 2015; accepted 14 February 2015
Available online 3 March 2015

Abstract

This paper presents the development of nanoparticulate indium tin oxide (ITO) inks for the continuous manufacture of ultrathin (~280 nm) ITO layers on PET substrates by roller coating at very high coating speeds. Ethanol- and water-based ITO inks containing polyvinylpyrrolidone as binder were prepared and rheologically characterized. The influence of different ink compositions on coating properties was evaluated by the concept of the dimensionless capillary number Ca. The ITO films were characterized concerning optical and electrical properties in dependence on ink composition and coating parameters. The organic solvent ethanol could be replaced by water, being cheap and environmental friendly. These inks allow the manufacture of sub-μm thin ITO layers with high layer quality and low specific electrical resistance of 3 Ω cm. Flexible and highly transparent ITO films with an inline-transmission of 88% in the regime of visible light which absorbed simultaneously up to 96% in the NIR region were produced.

Keywords: ITO; Nanopowder; Polyvinylpyrrolidone (PVP); Roller coating

1. Introduction

Transparent conductive oxides (TCOs) as indium tin oxide (ITO) or zinc oxide offer as a unique property simultaneously high electrical conductivity and high transparency [1]. They find application as transparent electrode materials in displays, touch screens or solar cells [2]. Conventionally, expensive vacuum-based sputtering techniques are used for the manufacturing of nanometer thin TCO layers [3,4]. Besides costs, sputtered TCO layers are brittle and therefore unsuitable for the use in flexible devices [5]. Printing and coating techniques based on nanoparticulate TCO materials can overcome both problems. Material-wise, such printed or coated films are composites of TCO particles and polymers manufactured at ambient atmosphere and room temperature offering high mechanical flexibility.

In the past, a large number of printing and coating techniques was developed to satisfy product requirements concerning design and functionality, e.g., inkjet printing is suitable for direct structuring [5–10] whereas coating techniques as spin coating [11] tape casting [12] or the profile rod technique [13] result in planar layers only. Rotary printing combines the advantages of both techniques; it offers the possibility to print both, planar layers and/or structures. Compared to inkjet printing or tape casting, rotary printing offers the additional advantage of a high throughput based on printing velocities of several hundred meters/min. It can be distinguished between four basic types of rotary printing techniques [14], like gravure printing, flat printing, relief printing, and screen printing. For the manufacture of fine-line electrical circuits from silver pastes on ceramics, direct gravure printing, allowing high resolutions of around 20 μm (line width) was developed [15]. Gravure printing of UV-curable nanoparticulate ITO inks for the manufacture of transparent electrodes has already been presented in the past [16–18]. Al-Dahoudi et al. also used UV-curable ITO inks to produce ITO layers by spin, dip and spray coating processes with a thickness of around 500 nm and a sheet resistance of 5 kΩ/□ [19]. Puetz et al. manufactured fine line patterns from nanoparticulate ITO inks with thicknesses between 0.2 and >1 μm and feature sizes in the range of 100 μm, at printing speeds of 40 m/min, using UV-curable ITO inks [16]. The resistance of the printed layers was decreased by UV illumination and heat treatments between 130 and 180 °C

* Corresponding author. Tel.: +49 91318527547.
E-mail address: andreas.roosen@fau.de (A. Roosen).

http://dx.doi.org/10.1016/j.jeurceramsoc.2015.02.012
0955-2219/

J Mater Sci (2015) 50:6124–6133
DOI 10.1007/s10853-015-9168-9

PVP a binder for the manufacture of ultrathin ITO/polymer nanocomposite films with improved electrical conductivity

Moritz Wegener[1] · Minato Kato[2] · Ken-ichi Kakimoto[2] · Stefanie Spallek[3] · Erdmann Spiecker[3] · Andreas Roosen[1]

Received: 24 March 2015 / Accepted: 8 June 2015 / Published online: 19 June 2015

Abstract This paper presents the manufacture of ultrathin (<1 μm) transparent conductive indium tin oxide (ITO) films based on nanoparticulate ITO slurries by the profile rod technique using the binder polyvinyl pyrrolidone (PVP) as an organic additive. The influence of the slurry composition on the film thickness and the specific electrical resistance as well as the transmission of the dried films is evaluated. The organic solvent ethanol and different types of the PVP binder were tested for slurry preparation and layer performance. ITO green films with low specific electrical resistance of 3 Ω cm, 87 % inline transmission, and layer thicknesses of only 250 nm could be manufactured. Furthermore, the influence of heat treatments up to 400 °C on the electrical properties of the ITO films was evaluated.

Introduction

Transparent conductive oxide (TCO) materials, e.g., indium tin oxide (ITO) or zinc oxide (ZnO), are of essential importance as transparent electrode materials in flat panel displays [1–4]. TCO materials combine high electrical conductivity and high optical transparency [1–5]. Rather brittle TCO layers are produced by conventional cost-intensive physical vapor depositions (PVD) and chemical vapor deposition (CVD) processes [6, 7]. Printing and coating techniques based on nanoparticulate materials could overcome the disadvantages named above [8]. In recent years, different printing and coating techniques, e.g., tape casting, spin coating, slot die coating, roller coating, and inkjet printing [9–14], have been the focus of research as methodologies for the deposition of nanoparticulate ITO-based systems. Typically, the dispersions or suspensions used contain organic compounds such as dispersing agents and binders, which improve particle dispersion during deagglomeration and particle adhesion after drying of the deposited layers, respectively. One drawback of such nanoparticulate ITO systems is that without any post-treatment they exhibit low conductivity due to poor electrical contact between the primary particle aggregates and high inter-grain porosity [8, 15, 16]; the charge carrier transport is additionally reduced by envelopment of the particles by the organic additives. In general, the electrical conductivity of nanoparticulate ITO films is based on fluctuation-induced tunneling between the ITO agglomerates [15, 17]. Gross et al. investigated different post-treatment methods to improve the conductivity of spin-coated nanoparticulate ITO layers, manufactured from commercial ITO dispersions, with layer thicknesses between 800 and 2500 nm. The best results were obtained by infiltration of a spin-coated porous ITO film with an ITO sol–gel precursor; the precursor was then converted to ITO thus filling the voids in the porous ITO network. Subsequent annealing at 550 °C in vacuum led to conductivities of 121 Ω^{-1} cm^{-1} [18]. Königer et al. showed that the electronic properties of nanoparticulate ITO

✉ Andreas Roosen
Andreas.roosen@ww.uni-erlangen.de

[1] Department of Materials Science, Glass and Ceramics, University of Erlangen-Nuremberg, Martensstr.5, 91058 Erlangen, Germany

[2] Department of Materials Science and Engineering, Graduate School of Engineering, Nagoya Institute of Technology, Gokiso-cho, Showa-ku, Nagoya 466-8555, Japan

[3] Center for Nanoanalysis and Electron Microscopy (CENEM), University of Erlangen-Nuremberg, Cauerstr. 6, 91058 Erlangen, Germany

Key Engineering Materials Vol. 672 (2015) pp 47-59
© (2015) Trans Tech Publications, Switzerland
doi:10.4028/www.scientific.net/KEM.672.47

Submitted: 2015-02-04
Revised: 2015-05-29
Accepted: 2015-05-29

Single nanogranules preserve intracrystalline amorphicity in biominerals

Stephan E Wolf[1, a *], Corinna Böhm[1,b], Joe Harris[1,c], Myriam Hajir[2,d], Mihail Mondeshki[2,e] and Frédéric Marin[3,f *]

[1] Friedrich-Alexander-University Erlangen-Nürnberg, Department of Materials Science and Engineering, Institute of Glass and Ceramics, Martensstrasse 5, 91058 Erlangen, Germany

[2] Institute of Inorganic and Analytical Chemistry, Johannes Gutenberg-University of Mainz, Duesbergweg 10-14, Germany

[3] UMR CNRS 6282 Biogéosciences, Université de Bourgogne, 6 Boulevard Gabriel, Dijon, France

[a] stephan.e.wolf@fau.de, [b] corinna.boehm@fau.de, [c] joe.harris@fau.de, [d] hajir@uni-mainz.de, [e] mondeshk@uni-mainz.de, [f] frederic.marin@u-bourgogne.fr

* To whom correspondence should be addressed.

Keywords: mollusk shell, *Glycymeris glycymeris*, *Pinna nobilis*, calcium carbonate, biomineralization, nanogranular, mesocrystal.

Abstract. We revisit the ultrastructural features of different calcareous biominerals and identify remarkable similarities: taxonomically very distant species show a common nanogranular structure, even if different extracellular secretion patterns are employed or calcium carbonate polymorphs formed. By these analyses, we elucidate the locus of the small fraction of intracrystalline organic matrix revealing its intergranular character and localize the intracrystalline amorphous calcium carbonate moiety commonly found in mesocrystalline biominerals and provide a first explanation for the pathway by which it is preserved.

1. Introduction

In the past decade, numerous elaborate studies investigating biomineral formation and structure have challenged classical concepts of crystallization and altered our view on both *in vivo* and *in vitro* crystallization. Although biominerals are mainly composed of simple and sparingly soluble inorganic salts such as calcium carbonate, they exhibit remarkable adaptations dependent on their specific task—be it as sensory organs as in the calcitic microlenses of brittlestars [1] or as exoskeletal protection in clam shells and sea urchins [2]. Since the Cambrian explosion marking the advent of biocalcification controlled by living organisms, an impressive number of calcifying species have developed. Prominent within this group are mollusks due to their remarkable diversity: roughly 85000 species are extant today and inhabit very different environments [3]. In spite of this taxonomical diversity, the microstructures of calcareous shells can be classified into seven main types from which the best-known, and important representatives, are the prismatic, the nacreous and the crossed-lamellar structures [4]. These seven microstructures are often combined in a consistent set within a given taxonomical order; prismatic layers are typically followed by nacre (*e.g.* in the order Pterioida) or crossed lamellar layers by complex crossed-lamellar regions (*e.g.* in the order Arcoida). A thorough understanding of the formation mechanism by which these different mollusk shell types and the calcareous skeletal elements of sea urchins are produced is still lacking. Sea urchin spines show an eye-caching, sponge-like, bicontinuous structure comprising curved surfaces. Each element behaves like a single crystal under polarized light or in X-ray and backscattered electron diffraction [5, 6]. Although taxonomically considerably separate, the calcified tissues of sea urchins and mollusks share astonishing similarities. First and foremost, they have both been shown to be formed by deposition of an amorphous transient phase. For sea urchins, it was recently shown in detail that two different forms of amorphous calcium carbonate (ACC) are actually involved during the mineralization process: initially a highly hydrated amorphous calcium carbonate is deposited that first has to dehydrate before it can finally crystallize [7, 8]. Surprisingly,

DENTAL MATERIALS 31 (2015) 293–301

Available online at www.sciencedirect.com

ScienceDirect

journal homepage: www.intl.elsevierhealth.com/journals/dema

Bulk-fill resin composites: Polymerization properties and extended light curing

José Zorzin[a,*], Eva Maier[a], Sarah Harre[a], Tobias Fey[b], Renan Belli[a], Ulrich Lohbauer[a], Anselm Petschelt[a], Michael Taschner[a]

[a] Dental Clinic 1 – Operative Dentistry and Periodontology, Friedrich-Alexander University of Erlangen-Nuernberg, Glueckstr. 11, D-91054 Erlangen, Germany

[b] Department of Materials Science and Engineering, Institute of Glass and Ceramics, Friedrich-Alexander University of Erlangen-Nuernberg, Martensstr. 5, D-91058 Erlangen, Germany

ARTICLE INFO

Article history:
Received 9 April 2014
Received in revised form
7 November 2014
Accepted 16 December 2014

Keywords:
Bulk-fill
Resin composites
Shrinkage stress
Volume shrinkage
Degree of conversion
Irradiance
Vickers hardness
FTIR spectroscopy

ABSTRACT

Objectives. The aim was to evaluate the polymerization properties of bulk-fill resin composites using two different light-curing protocols, in terms of degree of conversion (%DC), Vickers hardness (HV), polymerization volume shrinkage (PVS) and polymerization shrinkage stress (PSS) and compare them to conventional condensable and flowable resin composites.

Materials and methods. Filtek BulkFill (FBF, 3MESPE, Germany), SDR (Dentsply, Germany), TetricEvoCeram BulkFill (TBF, Ivoclar-Vivadent, Liechtenstein), Venus BulkFill (VBF, Heraeus, Germany), X-traBase (XTB, Voco, Germany), FiltekZ250 (3MESPE) and Filtek Supreme XTE Flowable (FSF, 3MESPE) were investigated. Light-curing was performed for 30 s or according to manufacturers' instructions (1200 mW/cm², Bluephase20i, Ivoclar-Vivadent). For %DC and HV, discs ($n = 5$) of 2 or 4 mm in thickness were prepared and stored for 24 h in distilled water at 37 °C. %DC was determined by FTIR-ATR-spectroscopy. %DC and HV were measured at the top and bottom of the specimens. PVS was measured using Archimedes method ($n = 6$). PSS measurements ($n = 10$) were carried out using 5 mm diameter PMMA rods as bonding substrates with a specimen height of 1 mm in a universal testing machine. Data were analyzed using one- and two-way ANOVA ($\alpha = 0.05$).

Results. Except Z250 in the manufacturers' light-curing mode, all materials showed no significant inferior %DC at 4 mm thickness. When light cured for 30 s Z250 had no significant differences in %DC at 2 or 4 mm when compared to top. FBF, TBF, FSF and Z250 displayed significant reduced HV at 4 mm in both curing modes. Z250 and TBF showed the lowest PVS and FSF the highest PSS in both curing modes.

Significance. All investigated bulk-fill composites obtained sufficient polymerization properties at 4 mm depth. Enhanced curing time improved the investigated polymerization properties of bulk-fills and Z250.

* Corresponding author. Tel.: +49 9131 8536479; fax: +49 9131 8533603.
E-mail address: zorzin@dent.uni-erlangen.de (J. Zorzin).

http://dx.doi.org/10.1016/j.dental.2014.12.010
0109-5641/

Proceedings

R. Hammerbacher, B. Dermeik, N. Travitzky, F. Lange, A. Roosen

Novel multilayer refractories derived of cast ceramic green tapes and preceramic papers

Proceedings of the 14th Biennial Worldwide Congress on Refractories UNITECR, 15-18 September 2015, Vienna, Austria, Ed.: UNITECR2015, USB-Stick, ISBN 978-3-9815813-1-7, 2015, No. 74, 4 pp

D. Jakobsen, A. Roosen

Generation of Residual Stresses in Multilayer Refractory Structures via Shrinkage Mismatch

Proceedings of the 14th Biennial Worldwide Congress on Refractories UNITECR, 15-18 September 2015, Vienna, Austria, Ed.: UNITECR2015, USB-Stick, ISBN 978-3-9815813-1-7, 2015, No. 203, 4 pp

M. Wegener, D. Spiehl, F. Mikschl, X. Liu, A. Roosen

Printing of Ultrathin Nanoparticulate Indium Tin Oxide Structures

Proceedings 11th International Conference and Exhibition on Ceramic Interconnect and Ceramic Microsystems Technologies, 20-23 April 2015, Dresden, Germany, Ed.: IMAPS, Washington, D.C., USA, 2015, 92-102

Books

M. Wegener, M. Lenhart, A. Roosen

Preparation of nanoscale powder for manufacturing TCO layers with high electrical conductivity and optical transparency

In: Technische Keramische Werkstoffe, J. Kriegesmann (Hrsg.), HvB Verlag, Ellerau, Kap. 3.3.3.10 (2015) 1-21

3. TEACHING

The Department of Materials Science and Engineering offers Bachelor and Master programmes in Materials Science and Engineering and in Nanotechnology.

The Bachelor course is a three years programme (six semesters) which qualifies for the Master programme (four semesters). The curriculum consists of the "*Grundstudium*" (basic studies) during the first 2 years, devoted to the fundamental scientific education. It introduces the student very early into materials science and engineering concepts by offering courses on materials structures, properties, thermodynamics, kinetics, chemistry, processing, product manufacturing, analysis and testing as well as practical training. Examinations follow immediately after each semester.

The subsequent advanced programme in the 5^{th} and 6^{th} semester broadly deepens the entire field of materials science and engineering. Courses on economics, management and other soft skills are obligatory. This period ends with a Bachelor Thesis of nine weeks duration. Additionally, the student has to perform an industrial internship of 12 weeks.

The Master programme in the 7^{th}, 8^{th} and 9^{th} semester specializes in a selected "*Kernfach*" (core discipline), including corresponding practical courses, seminars and courses in materials computational simulation. In addition the students select a *"Nebenfach"* (minor subject) from the Department of Materials Science and a *"Wahlfach"* (elective subject) from other Departments of the University, which offers the possibility of specialization. Finally, the programme is completed by a Master Thesis of six month duration.

In addition to this Materials Science and Engineering programme, the Institute of Glass and Ceramics is involved in the Bachelor and Master programmes “Energy Technology”, “Medical Technology” and the Elite course “Advanced Materials and Processes”.

a. Courses

(L) = lecture, (E) = exercise

1st Semester

- Introduction to Inorganic Non-metallic Materials (L); P. Greil
- Materials Science I (MB) (L); N. Travitzky (WS 14/15), K.G. Webber (WS 15/16)

2nd Semester

- Materials Science (CBI and CEN) (L); T. Fey
- Materials Science II (MB); N. Travitzky

4th Semester

- Basics in Programming (L/E); T. Fey, E. Bitzek

5th Semester

- Glass and Ceramics (L); A. Roosen (WS 14/15), D. de Ligny, K.G. Webber (WS 15/16)
- Instrumental Analytics (L); U. Deisinger (WS14/15), B. Kaeswurm (WS 15/16)
- Nanocomposites (L/E); T. Fey

7th to 9th Semester

- Physics and Chemistry of Glasses and Ceramics I: Thermodynamics of Condensed Systems (L); P. Greil
- Physics and Chemistry of Glasses and Ceramics II: Physicochemical Principles of Non-Crystalline Materials (L); D. de Ligny
- Structure and Properties of Glasses and Ceramics I: Electrical and Magnetic Properties (L); A. Roosen (WS 14/15), K.G. Webber (WS 15/16)
- Structure and Properties of Glasses and Ceramics II: Optical Properties (L); D. de Ligny
- Structure and Properties of Glasses and Ceramics III: High Temperature Properties (L); P. Greil
- Structure and Properties of Glasses and Ceramic IV: Mechanoceramics (L); P. Greil

- Functional Ceramics: Processing and Applications (L); A. Roosen (WS 14/15), K.G. Webber (WS 15/16)
- Glasses and Ceramics for Energy Technology, (L); D. de Ligny
- Glass Ceramics (L); D. de Ligny
- Glass Formulation (L); D. de Ligny
- Vibrational and Optical Spectroscopy of Glasses and Ceramics (L); D. de Ligny
- Biomimetic Synthesis of Materials (MAP) (L); S.E. Wolf
- Ceramic Materials in Medicine (L); S.E. Wolf
- Innovative Processing Techniques for Advanced Ceramic Materials (L); N. Travitzky
- Silicate Ceramics (L); N. Travitzky
- Powder Synthesis and Processing (L); S.E. Wolf
- Stresses and Mechanical Strength (L/E); T. Fey
- Computational Calculation of Crack Probabilities (E); T. Fey
- Non-Destructive Testing (E); T. Fey
- Mechanical Testing Methods (E); T. Fey

b. Graduates

Bachelor Thesis

Anja Briglmeir

Influence of the layer sequence on the sintering behavior and mechanical properties of multilayer structures from tape cast refractories

Theresia Derfuß

Preparation of fiber-reinforced polymer derived ceramics by electrophoretic deposition

Jannik Dippel

Influence of selected casting parameters on the strength, dimensional accuracy and surface quality in the manufacture of hot chamber casting salt cores

Anh-Dai Dang

Development of coating processes based on liquid-phases for manufacturing nanostructured surfaces

Simon Leupold

Imitation of biomimetic crystallization processes by the combination of low-molecular weight additives

Simon Roland

Manufacturing of syntactic foams

Christian Schmidt

Treatment of high-melting ternary refractory carbides for self-healing ceramics

Dorothea Wenzel

Ultralow frequency spectroscopy of glasses

Master Thesis

Werner Aumayr

Influence of the redensification on the mechanical properties of 3D printed ceramics

Martina Gayduschek

In situ characterization of carbonate-based precipitation reactions

Stefan Julmi

Manufacturing of boron carbide-containing composites by 3D printing

Joachim Knerr

High temperature properties of ordered lattice structures

Tobias Kranz

Screen printing on pre-ceramic papers

Johanna Schmidt

Piezoelectric materials for bioactive hybrid applications

Ph.D. Thesis

Robert Bathelt

Accelerated processing route for donor-doped potassium sodium niobate based piezoceramics

Armin Dellert

Anisotropies in film casting: particle orientation, drying stresses and shrinkage anisotropies

Tanja Einhellinger

Influence of spray-frozen and spray-dried granule properties on the quality of derived sintered bodies

Hans Windsheimer

Preparation and properties of multilayer ceramics from preceramic papers

4. ACTIVITIES

a. Conferences and Workshops

T. Fey

Member of the Program Committee and Session Chair of the 90th DKG Annual Conference & Symposium on High-Performance Ceramics of the Deutsche Keramische Gesellschaft, Bayreuth, Germany, 15-19 March 2015

T. Fey

Member of the organizing committee of the 39th ICACC Conference, Daytona Beach, Florida, USA, 25-30 January 2015

T. Fey

Member of the organizing committee of the 11th International Conference on Ceramic Materials and Components for Energy and Environmental Applications, 14-19 June 2015, Vancouver, Canada

D. de Ligny

Coordinator of the session "Glass heterogeneities and structural relaxation" at the "Glass & Optical Materials Division and Deutsche Glastechnische Gesellschaft", Joint Annual Meeting, Miami, Florida, USA, 17-21 May 2015

A. Roosen

Member of the Program Committee and Session Chair of the 90th DKG Annual Conference & Symposium on High-Performance Ceramics of the Deutsche Keramische Gesellschaft, Bayreuth, Germany, 15-19 March 2015

A. Roosen

Session Chair "LTCC Processing and Manufacturing" of the 11th International Conference and Exhibition on Ceramic Interconnect and Ceramic Microsystems Technologies, Dresden, Germany, 20-23 April 2015

A. Roosen

Organization of the 8th Advanced Training Course on „Tape Casting and Slot-Die Casting as well as Aspects of Multilayer Processing", University of Erlangen, Erlangen, Germany, 24-25 February 2015

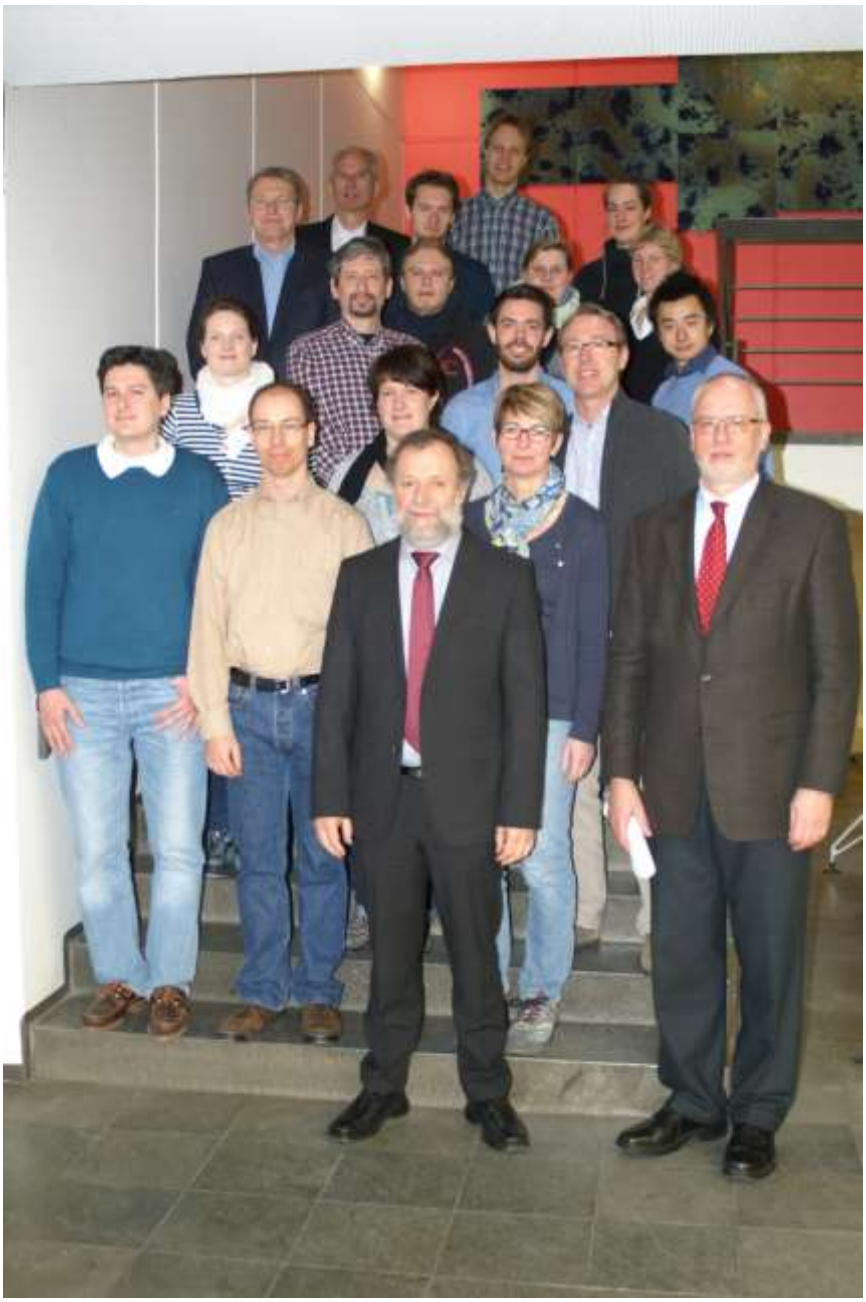

Members of the 8th Advanced Training Course on „Tape Casting and Slot-Die Casting as well as Aspects of Multilayer Processing"

Science Night

Science Night (Lange Nacht der Wissenschaften) on 24 October 2015 involved a large number of institutes in the region of Erlangen, Fuerth and Nuremberg. From 6 pm up to 1 am the Department of Materials Science opened the lab doors to show interested public exclusive experiments and latest research results in a common way.

The Chair of Glass and Ceramics presented the following attractions:

- 3D-movie with red/green glasses on cellular ceramic structures
- Ceramic sensors are hidden in many everyday objects: The driving skills of visitors could be demonstrated using ceramic sensors
- The original location of the famous crime series "Tatort" was shown.

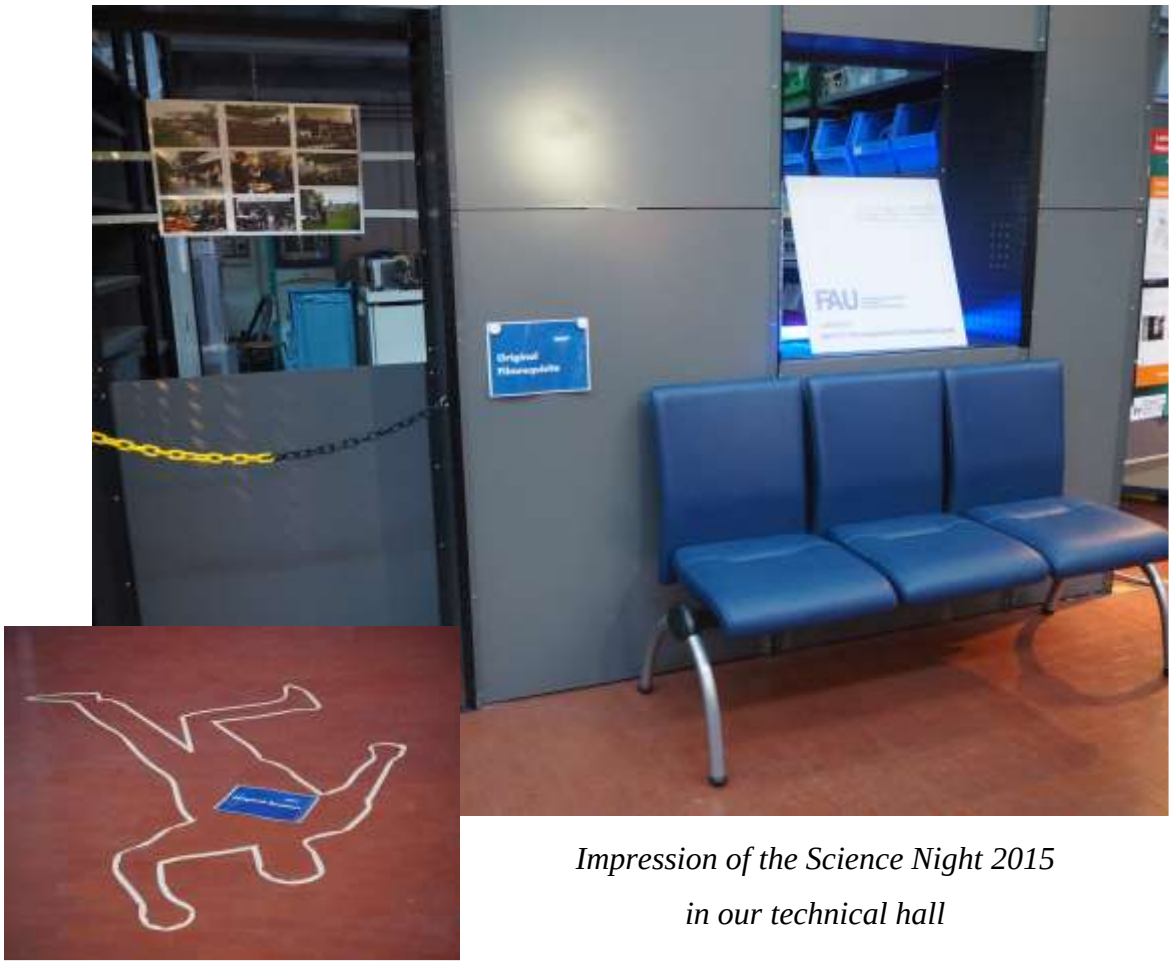

Impression of the Science Night 2015
in our technical hall

b. Invited Lectures

M.R. Cicconi

Redox Processes in Silicate Melts

2015 AGU Fall Meeting, San Francisco, USA, 14-18 December 2015

U. Deisinger, H. Sachsenweger, A.R. Boccaccini, R. Detsch

Biomedical application of tape cast $BaTiO_3$: in vitro biocompatibility evaluation of mesenchymal stem cells

14th International Conference of the European Ceramic Society, Toledo, Spain, 21-25 June 2015

T. Fey

Porous and cellular ceramics

AIST Nagoya, Japan, 17 February 2015

T. Fey, M. Götz, B. Diepold, P. Greil

Cellular Ceramic – Polymer Composites of Ceramic Building Blocks

4th International Symposium on Ceramics Nanotune Technology, Nagoya Institute of Technology, Nagoya, Japan, 2-4 March 2015

T. Fey

Preparation, characterization and simulation of porous materials

Seminar at the Otto Schott Institute of Materials Research (OSIM) at the Friedrich Schiller University of Jena, Jena, Germany, 1 July 2015

T. Fey

Ceramics for energy applications

Energy Materials Tutorials at Materials Weekend Warsaw, Warsaw, Poland, 19-20 September 2015

T. Fey

Porous Ceramics

Nagoya Institute of Technology, Nagoya, Japan, 25 November 2015

P. Greil

Surface Healing of Polymer-Filler Derived Ceramic Matrix

Chinese-German Symposium, Darmstadt, Germany, 28 July 2015

D. Jakobsen,I. Götschel, A. Roosen

Manufacture of multilayered refractory composites by tape casting with optimized thermal and chemical properties

DFG closing event of the Priority Programme SPP 1418 „FIRE“, Freiberg,Germany, 8-9 December 2015

D. de Ligny, A. Posch, F. Kalkowski, J. Ernst, A. Nowak, D.R. Neuville, A. Lenhart

Using Prince Rupert’s drops to induce extreme tensile stress in glasses, a Raman spectroscopy study

GOMD-DGG 2015 Joint Annual Meeting, Miami, Florida, USA, 17-21 May 2015

D. de Ligny

Prince Rupert's drops a way to put glasses under extreme tensile stress

DGG Glasforum, Fulda, Germany, 2 October2015

D. de Ligny

Glasses at extreme conditions: Prince Rupert’s drops a fun way to induce extreme tensile stress in glasses

Institute of Mineralogy and Crystallography, University of Vienna, Austria, 30 October 2015

N. Travitzky, P. Greil

Additive manufacturing of ceramics

Welding, Joining and Additive Manufacturing, International Conference 2015, Tel Aviv, Israel, 18-20 January 2015

N. Travitzky, P. Greil

Additive manufacturing of ceramic-based composites

23rd European Dental Materials Conference, Nuremberg, Germany, 27-28 August 2015

N. Travitzky, P. Greil

Additive manufacturing of ceramics by extrusion freeform fabrication (EFF) and laminated object manufacturing (LOM)

Symposium on Additive Manufacturing – Process Engineering and Application in Ceramics, German Ceramic Society, Erlangen, Germany, 1-2 December 2015

N. Travitzky, P. Greil

Additive manufacturing of ceramic-based composites

The International Seminar on Interdisciplinary Problems in Additive Technologies, Problems of materials science in additive technologies, Tomsk, Russia, 16-17 December 2015

M. Wegener, D. Spiehl, A. Roosen:

Flexography Printing of Nanoparticulate Indium Tin Oxide Structures

14th International Conference of the European Ceramic Society, Toledo, Spain, 21-25 June 2015

S.E. Wolf

Bionics: Learning from Mother Nature.

Annual Meeting of the Natural Science Branch of the Konrad-Adenauer Foundation, Gersfeld, Germany, 03-05 July 2015

S.E. Wolf

A Classical View on a Nonclassical Crystallization Process: The PILP-Process Revisited

20th American Conference on Crystal Growth and Epitaxy (ACCGE-20), Big Sky, Montana, USA, 2-7 August 2015

B. Zierath, T. Fey, A. Kern, B. Etzold, P. Greil

Hierarchically Structured Silicon Carbide Derived Carbon Monoliths for Catalyst Support Structures

BaCaTec, HRL Labs, Malibu, USA, 2 February 2015

c. Awards

U. Deisinger, S. Hagen, A. Roosen

Cold Low Pressure Lamination for the Fabrication of Multilayer LTCC Structures with Internal Cavities

Second place in poster competition of the 90th DKG Annual Conference & Symposium on High-Performance Ceramics of the Deutsche Keramische Gesellschaft, Bayreuth, Germany, 5-19 March 2015

T. Fey

In March 2015 Dr. Tobias Fey was announced by the German Ceramic Society (DKG) as Leader of a new working team "TFA 6-1: Characterization of porous ceramics".

T. Fey

Dr. Tobias Fey was appointed to Associate Professor (note: equivalent to a Guest Visiting Prof) from Nagoya Institute of Technology (NITech), Department of Materials Science, for the years 2015-2019

P. Greil

Fellow of the European Ceramic Society,

14th International Conference of the European Ceramic Society, Toledo, Spain, 24 June 2015

5. ADDRESS AND IMPRESSUM

Department of Materials Science - Glass and Ceramics

Friedrich-Alexander University of Erlangen-Nuremberg

Martensstr. 5

91058 Erlangen, GERMANY

Phone: ++49-(0) 9131-852-7543 (Secretary)

Fax: ++49-(0) 9131-852-8311

E-mail: ww3@ww.fau.de

Internet: http://www.glass-ceramics.fau.de/

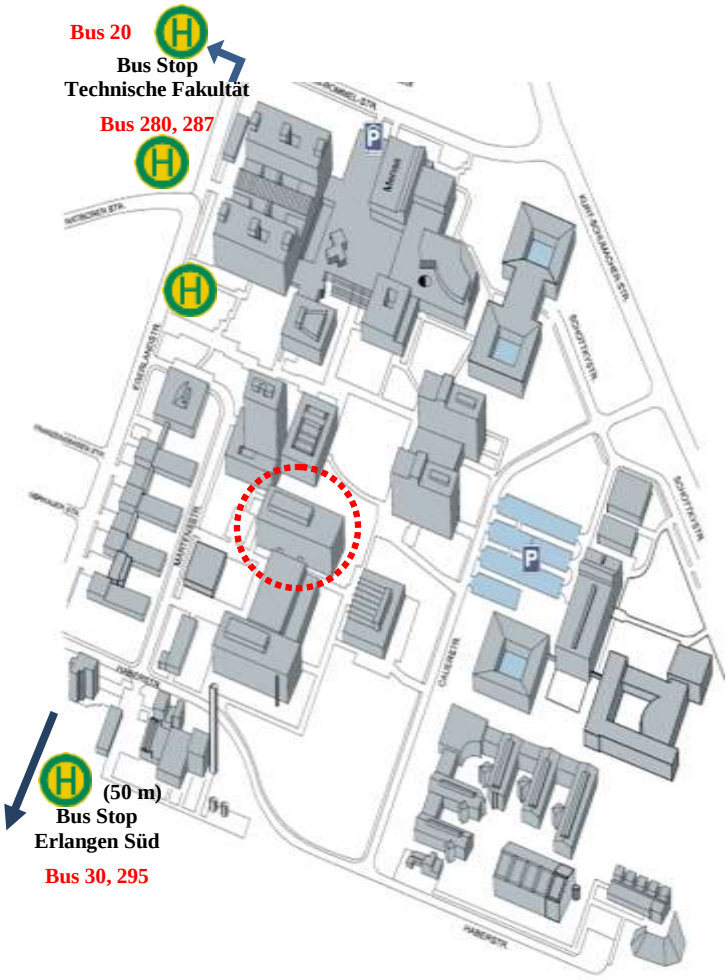

By car:

Highway A3 exit **Tennenlohe**; direction to Erlangen (B4).

Follow the signs "**Universität Südgelände**".

After junction "**Technische Fakultät**" please follow the map.

By train:

Railway station **Erlangen**.

Bus line No. 287 direction "**Sebaldussiedlung**".

Bus Stop "**Technische Fakultät**".

50 meters to a layout plan; search for "**Department Werkstoffwissenschaften**".

http://www.glass-ceramics.fau.de/contact/maps/

Center for Advanced Materials and Processes (ZMP)

Dr.-Mack-Strasse 81

Technikum, Ebene 3

D-90762 Fürth

Tel.: ++49-(0) 911-950918-10

Fax: ++49-(0) 911-950918-15

Internet: http://www.zmp.fau.de/

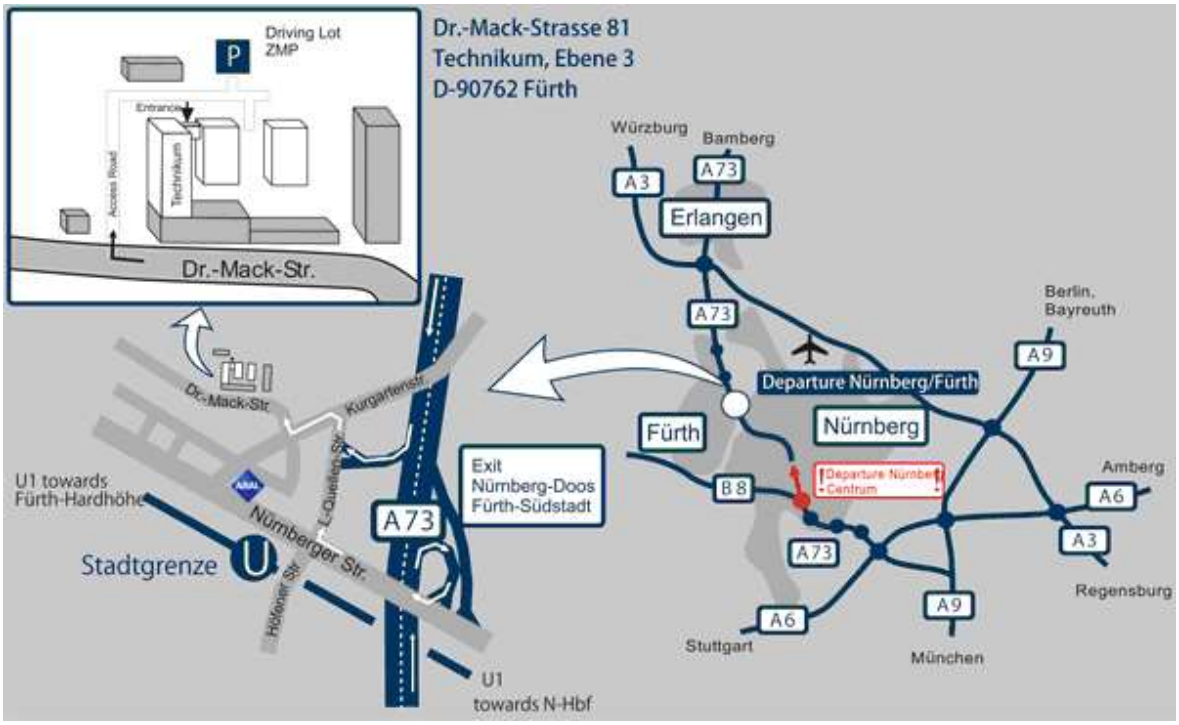

http://www.zmp.fau.de/anfahrt/

Impressum

Prof. Dr. Peter Greil

Dr. Andrea Dakkouri-Baldauf

Department of Materials Science – Institute of Glass and Ceramics

Martensstraße 5

91058 Erlangen, GERMANY